PhD thesis
Synthesis and Application of Electron Transporting Polymer for Electroluminescent and Photorefractive Applications

Mototora Kai

(Yuanhu Pei)

Graduate School of Bio-Applications and Systems Engineering,

Tokyo University of Agriculture and Technology

August 2023

Chapter 1 General Introduction

1.1 Organic Semiconductors

It has long been known that molecular crystals of condensed polycyclic aromatic compounds such as anthracene conduct electricity. Akamatsu and Iguchi et al. named these compounds organic semiconductors [1]. In 1959, poly(*N*-vinylcarbazole) (PVK), the first polymer to be utilized, was reported to exhibit photoconductivity, which is one of the properties of semiconductors[2, 3]. The hole mobility of PVK is 10^{-6} to 10^{-7} cm^2 V^{-1} sec^{-1}, which is significantly smaller than that of anthracene single crystal (~1 cm^2 V^{-1} sec^{-1}). The image that the mobility is extremely small in amorphous polymers was established. However, from a practical point of view (processability, visible light transparency), there is a great demand for amorphous materials. In molecular dispersed systems, charge transport materials with low molecular mass are molecularly dispersed in inert binder polymers such as polystyrene and polycarbonate[4]. Polymeric materials consisting of single components are also very attractive because of high morphological and thermal stability.

Organic semiconductors are characterized by exhibiting photoconductivity and charge (hole or electron) transporting abilities Utilizing these characteristics, it is applied to electrophotography[5], organic electroluminescence (EL) devices[6], photovoltaic devices[7], photorefractive (PR) devices[8], and so on. Examples of polymeric semiconductors include π-conjugated polymers such as polythiophene and poly(phenylene vinylene), which generally exhibit strong absorption in the visible light region. On the other hand, many polymers containing units that exhibit charge transporting abilities as low molecules, such as triphenylamine (TPA) derivatives, are transparent in the visible light region, and are suitable for electrophotography, organic EL devices, and PR devices. The TPA site easily adopts a propeller-type conformation centered on N atoms, and in spite of a low-molecular molecule, it is difficult to crystallize and easily form an amorphous thin film. Therefore, in an organic EL device, an amorphous vapor-deposited thin film is used as it is as an active layer. In addition, when it is incorporated into the side chain or main chain of a polymer, unlike a planar carbazole ring, it does not form a dimer radical cation, preventing a decrease in mobility (dimers are energetically stable, become a trap site).

TPA derivatives have been classically synthesized by the Ullmann reaction using secondary aromatic amines and aryl iodides[9]. Generally, this reaction requires harsh conditions and an excess of relatively expensive iodide. In the latter half of the 1990s, a new C-N coupling reaction using a palladium catalyst was discovered, and the reaction conditions were mild and yields improved [10]. In this reaction, not only can a cheap bromide be used, but also it proceeds almost stoichiometrically, so many recent research examples use this method.

1.2 Carrier Transporting Mechanism

Characteristics such as photoconductivity and conductivity depend on how efficiently the carriers

generated in the organic semiconductor by light irradiation or injection from the electrode are transported through the material. Carrier transporting can be regarded as electron transfer between molecules of the same kind under an electric field as shown in Eq. 1-1. Drift transporting in amorphous solid systems such as amorphous polymers is thought to occur by a hopping mechanism through the overlap of π electron clouds between molecules.

$$\begin{matrix} M^{\dot{+}} + M^0 \\ M^{\dot{-}} + M^0 \end{matrix} \longrightarrow M^0 \qquad (1\text{-}1)$$

This is a one-electron redox process facilitated by heat and an electric field between a neutral molecule (M^0) and its radical cation ($M^{+\cdot}$) or radical anion ($M^{-\cdot}$). Hole transporting involves electron transfer from the highest occupied molecular orbital (HOMO), and electron transfer involves electron transfer from the lowest unoccupied molecular orbital (LUMO). By repeating this electron transfer reaction, the carriers move through the substance. The velocity at this time is represented by the drift mobility μ ($cm^2V^{-1}s^{-1}$). The average moving velocity v ($cm\ s^{-1}$) of the charged body is proportional to the electric field strength E ($V\ cm^{-1}$), and the proportional constant is the drift mobility. That is, the drift mobility is the average distance moved per unit time under a unit electric field strength.

Aromatic amines represented by TPA are susceptible to one-electron oxidation of the central nitrogen to form radical cations. In order for these radical cations generated by light-induced or electrode reactions to become chemical species responsible for hole transporting, they must have enough activity to oxidize adjacent neutral molecules and at the same time repeat reversible redox reactions. Simultaneously it must have stability that allows repeated reversible redox reactions.

1.3 Electron Transporting Materials

Electron-transporting materials enable positive-charging electrophotographic processes that generate a small amount of ozone during charging, and are essential components of the electron-transporting layer in organic EL devices. The development of electron-transporting materials has lagged behind that of hole-transporting materials. This is probably because the solubility and crystallinity of the electron-accepting compound with respect to the binder have been problematic because the studies have centered on the molecular dispersion system. Figure 1-1 shows the electron transporting materials mainly developed for electrophotography. Trinitrofluorenone (**1**) is an electron-transporting compound that has been known for a long time, and was once noted as an organic photoreceptor material[11]. Fluorene derivatives (**2**)[12], thiopyran derivatives (**3**)[13], diphenoquinone derivatives (**4**)[14], oxadiazole derivatives (**5**)[15], and so on have been reported. Polymers containing electron-transporting moieties in side-chains have also been synthesized to solve the phase separation problem. Fig. 1-1 shows an example of an electron-transporting side-chain polymer synthesized by

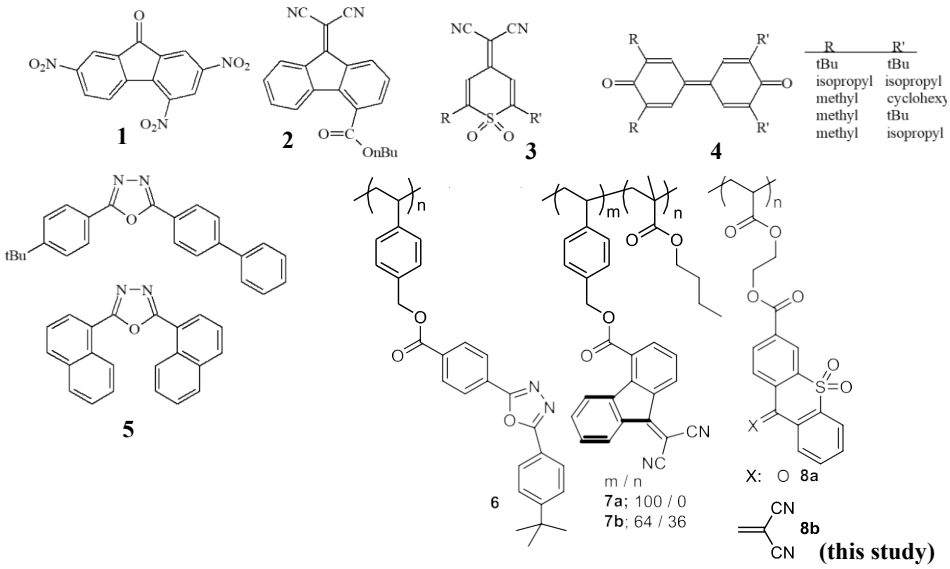

Fig.1-1 Typical electron transporting materials

the authors. Polymer **6** is used as an electron transport material for organic EL devices[16]. Polymer **7** in which a fluorene derivative is incorporated in the side chain was reported. The homopolymer **7a** has poor film-forming properties, but the copolymer **7b** with butyl methacrylate gives a good thin film. Higher mobility is observed in this thin film than in low-molecular-weight dispersions[17]. The electron mobility of polyacrylate **8** having thioxanthene derivatives in the side chains was investigated in this study.[18]

1.4 Electroluminescent Applications

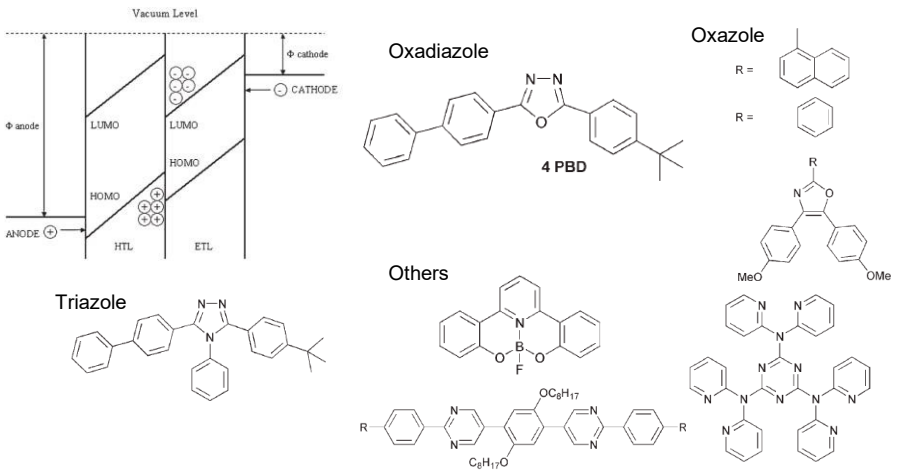

Fig.1-2 Electron transporting materials for electroluminescent device (low molecular mass)

A variety of low-molecular-weight materials were studied for organic electroluminescence devices such as oxadiazole[19], oxazole[20], and triazole[21]. Fig. 1-2 shows conceptual energy diagram of an organic EL device. A metal with a small work function is used as the cathode, and a material with a deep LUMO (electron-deficient) is used as the electron transport layer. In organic EL devices, the material is deposited by vacuum evaporation, and it is also necessary to design the material so that it does not crystallize easily.

A variety of polymeric materials have been developed as shown in Fig. 1-3. Polyfluorene derivatives have been extensively studied as a material system that has both electron-transporting and light-emitting properties.[22] The material on the upper-right was synthesized using a nucleophilic aromatic substitution reaction, taking advantage of the electron-withdrawing properties of a polyether containing an oxadiazole backbone that exhibits electron-transporting properties.[23] The two polymers below were designed not from the viewpoint of electron transporting, but rather from the viewpoint of their properties as light-emitting materials.[24, 25]

A white light-emitting material was obtained by copolymerizing an orange light-emitting unit, which is the complementary color of blue.[26] This is a block copolymer with a hole-transporting polymer, but it has an orange light-emitting site at the connecting part.[27] In principle, multi-layered structure in the device is desirable for the luminescent efficiency and it is difficult to fabricate because the polymeric devises are usually prepared using wet processes. Compared with the conventional

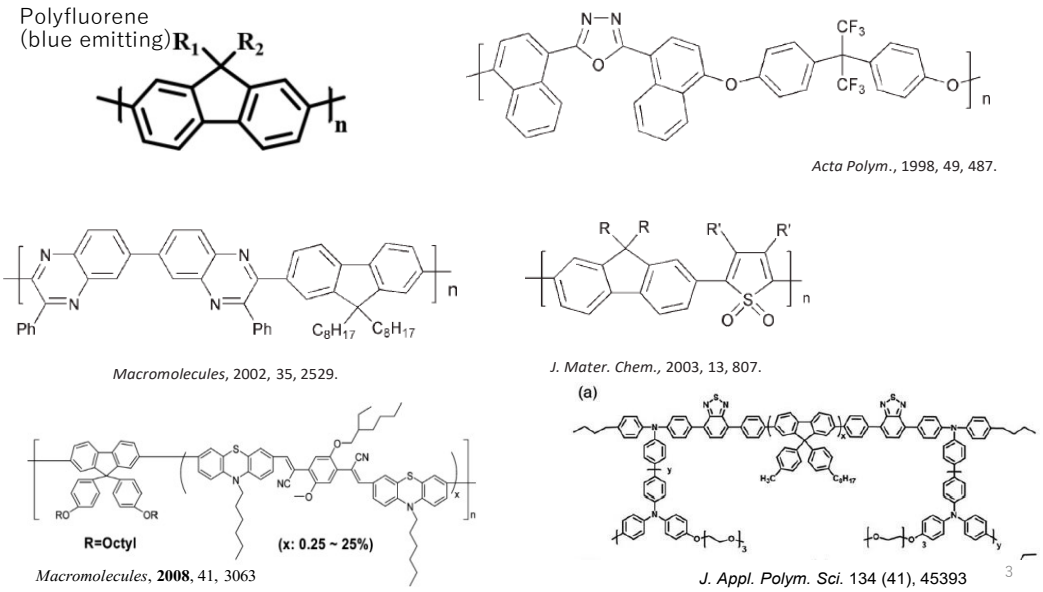

Fig. 1-3 Electron transporting polymers for electroluminescence

polymers, complex synthetic strategy is necessary.

1.5 Photorefractive Applications

It is generally accepted that a photorefractive effect involved four distinct processes: charge generation, charge transport, charge trapping, and index of modulation. As shown schematically in Figure 1-4 illustrates the basic process to generate the PR effect [28].

(a) Interference pattern and charge generation

Figure 1-4 (a) shows the optical wave pattern of beam intensity that is produced by two intersecting coherent beams. This interference pattern consists of light and dark region. At the light region, the separation of electrons and holes is occurred by the absorption of an incident photon.

(b) Charge transport by drift or diffusion

In Figure 1-4 (b), the holes are shown to be more mobile, which is the more common case for organic charge transporting materials. If both carriers are equally mobile, the resulting space-charge distribution could have zero internal electric field and hence no PR effect. The physical processes giving rise to charge transport are either diffusion due to density gradients, or drift: in the presence of an applied electric field. Since most polymeric materials are relatively good insulators, the ability of the charges to move by diffusion alone is quite limited. Therefore, it is generally believed that the drift is the dominant mechanism for charge transport.

(c) Trapping of carriers at the dark area, and non-uniform space charge distribution

The migrated carriers are trapped in the trapping centers, leading to a space charge distribution which corresponds to the interference pattern of beam intensity. Since this space charge distribution results in an electric field described by Poisson's equation the resulting the phase of space charge field is shifted in space by π /2 relative to that of the trapped charges.

(d) Formation of the space charge field, and modulation of the refractive index

The final process is the formation of the phase grating due to the space charge modulation of the refractive index via the linear electro-optical effect.

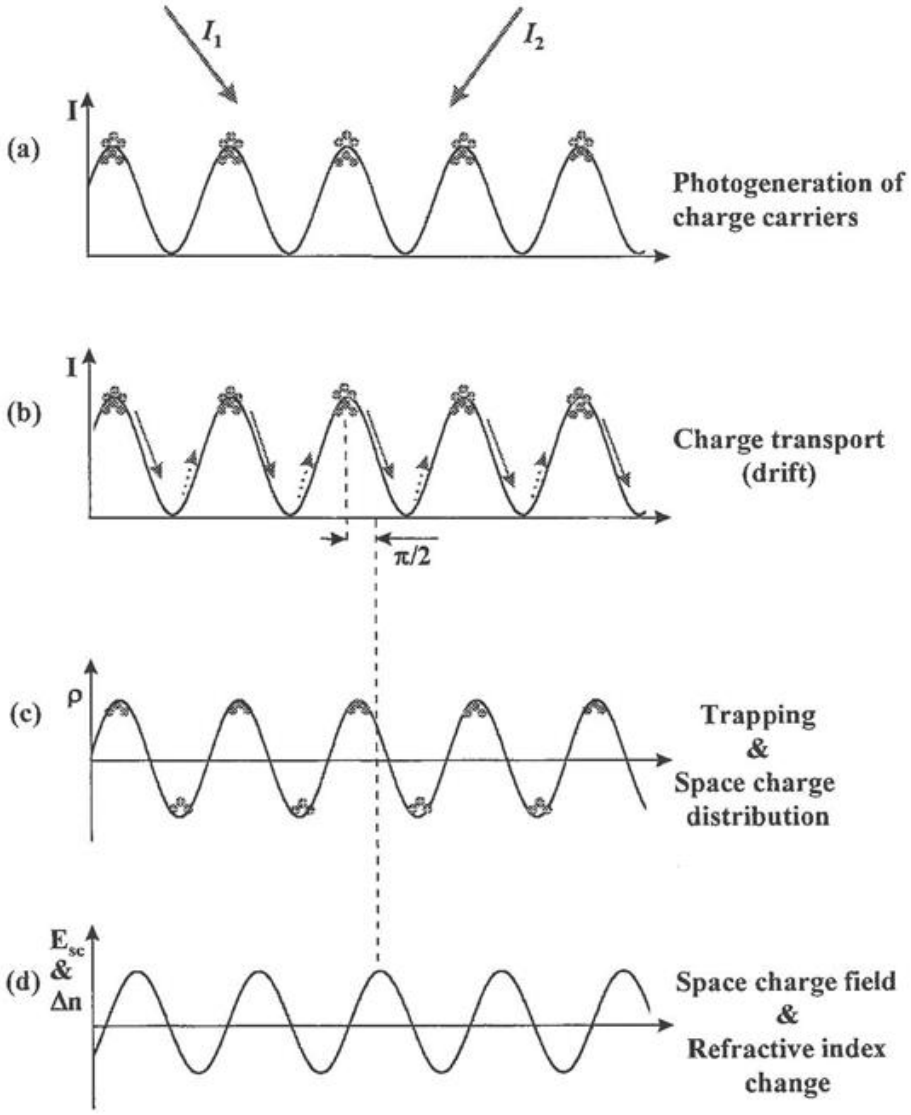

Fig. 1-4 Formation process of photorefractive grating.

High PR performance, such as high diffraction efficiency, large coupling gain, and fast response, has been observed for host-guest systems with low glass transition temperature (T_g) consisting of a photoconducting polymer as a host, an electo-optically (EO) active chromophore, and a small amount of a photosensitizer[29-38]. To lower *T*g, a plasticizer has been sometimes utilized. In these composite materials, large index modulation is believed to come primarily from orientational photorefractivity that is related to the polarizability anisotropy of the dopant chromophore[39].

As a photoconducting host polymer, hole-transporting (electron donating) polymers such as

poly(vinyl carbazole) (PVK)[30,36], polysiloxane containing carbazole unit[31], polyacrylate containing tetraphenyldiaminobiphenyl unit[32, 35], and poly(triarylamine)[33, 34, 37, 38] have been exclusively used. There is still a serious problem to be solved, *i.e.*, the crystallization or aggregation of EO chromophores limits the life time of PR devices.

In our research group electron transporting polymers were successfully synthesized[16-18], and first reported the PR composites consisting of an electron transporting host polymer, which is acrylate polymer containing thioxanthene derivative on the side chain (P-THEA), and EO active 4-*N,N*-diethylamino-β-nitrostyrene (DEANST)[40]. It was found that durability of PR devices greatly extended due to the better compatibility of P-THEA and DEANST. Enhanced compatibility was mainly attributed to the electrical interaction between electron accepting P-THEA and electron donating DEANST. This interaction also resulted in the absorption at 633 nm (He-Ne laser) although both P-THEA and DEANST are inherently transparent at that wavelength. The charge transfer interaction made photocharge generation possible without a photosensitizer. Although 64 cm^{-1} of two-beam coupling gain at 50 V/μm was obtained for P-THEA/DEANST (70/30), the net gain was only 31 cm^{-1} because of the large absorption. Therefore, it is important to utilize a host polymer that interacts electrically with EO chromophore to a lesser extent in order to fabricate an efficient PR device. Same phenomena were observed in PR molecular glass based on electron transporting acceptor and EO chromophore[41,42]. Polymers[43,44] and a molecular glass[45] containing thioxanthene moiety also possess unique optical properties exhibiting pseudo-PR characteristics without applied electric field governed by a different mechanism under limited conditions.

1.6 Purposes

There are still problems to be solved for improve the performance of electrophotography, electroluminescent, and photorefractive devises. It is necessary to develop electron transporting polymers with high transparency, and high electron mobility. For electroluminescent applications, simple synthetic strategies are desired from the practical point of view.

In this study, the author focused on the development of electron transporting polymers with high transparency based on thioxanthene moiety, and photorefractive application (Chapter 2, and 5). The author also tried to develop electron transporting polymers with hole transporting and luminescent ability via simple synthetic strategies (Chapter 3 and 4).

References

1) H. Iguchi, "*Yukihandotai*", Makishoten, Tokyo, 1964

2) H. Hoegel, O. Sus, W. Neugebauer, *German Patent* 1068115 (1959)

3) M. Stolka, D. M. Pai, D. S. Renfer, J. F. Yanus, *J. Polym. Sci., Polym. Chem. Ed*., **21**, 969 (1983)

4) (a) M. Stolka, J. F. Yanus, D. M. Pai, *J. Phys. Chem*., **88**, 4707 (1984); (b)T. Sasakawa, T. Ikeda, S.

Tazuke, *J. Appl. Phys*., **65**, 2750 (1989); (c) P. M. Borsenberger, *J. Appl. Phys.*, **68**, 5188 (1990); (d) Y. Kanemitsu, *J. Appl. Phys*., **71**, 3033 (1992)

5) P. M. Borsenberger, D. S. Weiss, "*Organic Photoreceptors for Imaging Systems*", Marcel Dekker, New York, 1993

6) (a) C. W. Tang, S. A. Vanslyke, *Appl. Phys. Lett*., **51**, 913 (1987); (b) S. Tokito, C. Adachi, H. Murata,"Yuki EL display" Ohmu-sha, Tokyo, 2004

7) (a) N. S. Sariciftci, L. Smilowitz, A. J. Heeger, F. Wudl, *Science*, **258,** 1474 (1992); (b) H. Hoppe, N.S. Sariciftci, *J. Mater. Rev*., **19,** 1924 (2004)

8) (a) W. E. Moerner, S. M. Silence, *Chem. Rev*., 94, 127 (1994); (b) S. J. Zilker, *ChemPhysChem*, **1**, 72 (2000)

9) Y. Shirota, T. Kobata, N. Noma, *Chem. Lett*., 1989, 1145

10) (a)J. Louie, M. S. Driver, B. C. Hamann, J. F. Hartwig, *J. Org. Chem*., **62**, 1268 (1997); (b) T. Yamamoto, M. Nishiyama, Y. Koie, *Tetrahedron Lett.*, **39**, 2367(1998)

11) W. D. Gill, *J. Appl. Phys*., **43**, 5033 (1972)

12) P. M. Borsenberger, T. M. Kung, W. B. Vreeland, *J. Appl. Phys*., **68**, 4100 (1990)

13) P. M. Borsenberger, W. T. Gruenbaum, *J. Polym. Sci., Part B.*, **34**, 575 (1996)

14) Y. Yamaguchi, H. Tanaka, M. Yokoyama, *J. Chem. Soc. Chem. Commun.*, **1990**, 222

15) H. Tokuhira, M. Era, T. Tsutsui, S. Saito, *Appl. Phys. Lett.*, **66**, 3433 (1995)

16) (a) H.Sato, Y. Sakaki, K. Ogino, Y. Ito, *Polym. Adv. Technol*., **8**, 454 (1997); (b) J.-M. Son, Y. Sakaki, K. Ogino, H. Sato, *IEEE Trans. on Electron Devices*, **44**, 1307 (1997)

17) (a) J.-H. Sim, K. Ogino, H. Sato, *Synth. Met.,* **69**, 575 (1995); (b) J.-H. Sim, K. Ogino, H. Sato, Y. Pei, *J. Imag. Sci. Technol.*, **40**, 164 (1996)

18) H. Sato, H. Matsuda, K. Okamoto, K. Ogino, *Synth. Met*., **105**, 55 (1999)

19) C. Adachi, T. Tsutsui, S. Saito, *Appl. Phys. Lett*. **56**, 799 (1990)

20) R. H. Jordan, A. Dodabalapur, M. Strukelj, T. M. Miller, *Appl. Phys. Lett*. **68**, 1192 (1996)

21) J. Kido, K. Hongawa, K. Okuyama, K. Nagai, *Appl. Phys. Lett*. **63**, 2627 (1993)

22) M. Fukuda, K. Sawada, K. Yoshino, *Jpn. J. Appl. Phys*. **28** L1433 (1989)

23) P. Pösch,R. Fink,M. Thelakkat,H.-W. Schmidt, *Acta Polymerica*, **49**, 487 (1998)

24) X. Zhan, Y. Liu, X. Wu, S. Wang, D. Zhu, *Macromolecules,* **35**, 2529 (2002)

25) M. Pasini, S. Destri, W. Porzio, C. Botta, U. Giovanella, *J. Mater. Chem.*, 13, 807 (2003)

26) M.-J. Park, J. Le, J.-H. Park, S. Kyu Lee, J.-Ik Lee, H.-Y. Chu, D.-H. Hwang, H.-K. Shim, *Macromolecules*, **41**, 3063 (2008)

27) K. Kim,Y. Inagaki, S. Kanehashi, K. Ogino, *J. Appl. Polym. Sci.* **134**, 45393 (2017)

28) W. E. Moerner and S. M. Silence, *Chem. Rev.*, **94**, 127 (1994).

29) N. Tsutsumi, *Polym. J.,* **42**, 572 (2016)

30) K. Meerholz, B. L. Volodin, Sandalphon, B. Kippelen, N. Peyghambarian, *Nature*, **371**, 497 (1994)
31) H. Chun, I. K. Moon, D.-H. Shin, N. Kim, *Chem. Mater.*, **13**, 2813 (2001)
32) K. Ogino, T. Nomura, T. Shichi, S.-H. Park, H. Sato, T. Aoyama, T. Wada, *Chem. Mater.*, **9**, 2768 (1997)
33) Z. Cao, Y. Abe, T. Nagahama, K. Tsuchiya, and K. Ogino, *Polymer*, **54**, 269 (2013)
34) N. Tsutsumi, K. Kinashi, K. Masumura, K. Kono, *Opt. Express,* **23**, 25158 (2015)
35) P.-A. Blanche, B. Lynn, D. Churin, K. Kieu, R. A. Norwood, N. Peyghambarian, *Sci. Rep.*, **6**, 29027 (2016)
36) H. Chiba, K. Hosoyama, R. Ogawara, S. Kanehashi, K. Ogino, *J. Fiber Sci. Technol.*, **74**, 215 (2018)
37) K.-L. Wang, J.-C. Jiang, C.-H. Jhu, S. Wada, T. Sassa, M. Horie, *J. Mater. Chem. C*, **8**, 13357 (2020)
38) N. Tsutsumi, S. Sakamoto, K. Kinashi, B. J. Jackin, W. Sakai, *ACS Omega*, **7**, 12120 (2022)
39) W. E. Moerner, S. M. Silence, F. Hache, G. C. Bjorklund, *J. Opt. Soc. Am. B*, **11**, 320 (1994)
40) K. Okamoto, T. Nomura, K. Ogino, H. Sato, *Chem. Mater.,* **11**, 3279 (1999)
41) J.-M. Jeong, H. Sato, J. Pretula, K. Kaluzynski, K. Ogino, *Jpn J. Appl.Phys., Part 1*, **42(4A)**, 1655 (2003)
42) J.-M. Jeong, K. Abe, H. Sato, J. Pretula, K. Kaluzynski, K. Ogino, *Synth. Met*. **139**, 11(2003)
43) H. Chiba, G. Wakamatsu, S. Kanehashi, K. Oigno, *J. Photopolym. Sci. Technol.*, **31**, 711 (2018)
44) H. Chiba, T. Murata, S. Kanehashi, K. Ogino, *J. Fiber Sci. Technol*., **74**, 202 (2018)
45) J.-M. Jeong, K. Ohnishi, H. Sato, K. Ogino, *Jpn. J. Appl. Phys., Part 2*, **42(2B)**, L179 (2003)

Chapter 2 Electron Transporting Polymers having Thioxanthene Derivatives

Abstract: Acrylate and methacrylate type monomers containing thioxanthene derivative were synthesized and radically polymerized to yield electron transporting polymers. The obtained polymers are soluble in common solvents such as tetrahydrofuran (THF), chloroform, dimethylformamide (DMF). Cyclic voltammograms of all polymers showed two well-defined pairs of reduction and oxidation peaks indicating that polymers are electrochemically active. The polymers with dicyanomethylated thioxanthene derivative were more easily reduced than those with unmodified one because of the strong electron-withdrawing effect of dicyanomethyl groups, while the latter showed higher electron drift mobility than the former. Drift mobility was discussed in relation to the structure of the lowest unoccupied molecular orbital (LUMO). and the electron distribution. A well-balanced distribution of electrons plays an important role for a high-mobility material.

2.1 Introduction

Charge transporting materials are used in many fields such as photoreceptors of electrophotography, organic electroluminescent devices, and photorefractive devices. Most of the charge transporting materials are low-molecular-weight compounds, which are used in cast films with binding polymers for electrophotography and photorefractive devices or vapor-deposited ultrathin films for electroluminescent devices. It is reported that low-molecular weight compounds easily crystallize or aggregate when they are vapor-deposited or highly dispersed in a polymer matrix[1,2]. Low-molecular-weight compounds also have poor mechanical strength. Therefore, polymeric materials are investigated to resolve these problems.

Charge transporting materials are divided into two groups: hole (HTM). and electron transporting materials (ETM). The former is easily subject to be oxidized and transports positive charges, and the latter accepts electrons easily and transports negative charges. Hitherto, HTMs have been intensively studied. However, only a few investigations have been done on ETM, including derivatives of fluorenone[3,4], oxadiazole[5,6], and thiopyran[7] in contrast with HTM, and no compounds with drift mobility or solubility in polymer comparable to those of HTM have been developed. Nagasawa et al. reported that thioxanthene derivatives have high electron mobility in the order of 10^{-6} cm^2/Vs, although they have high tendency to crystallize[8]. Research group the author belonged to have demonstrated that a charge-transporting chromophore can be highly introduced by polymerization of a vinyl type monomer containing a chromophore, and the resulting polymer shows excellent thermal and morphological stability[9–12]. In this chapter, polymers having the thioxanthene dioxide unit on a side chain were prepared and its electrical and electrochemical properties are studied.

1.2. Experimental

1.2.1. Materials

9-Oxo-9*H*-thioxanthene-3-carboxylic acid 10,10-dioxide was purchased from Aldrich and used as received. Malononitrile, 2-hydroxyethyl acrylate, 2-hydroxyethyl methacrylate, dicyclohexylcarbodiimide, 4-dimethylaminopyridine, 2-bromoethanol, acryloyl chloride, methacryloyl chloride, titanium (IV) chloride were purchased from Kanto Chemical and used without further purification. Solvents were purified by conventional distillation under a nitrogen atmosphere.

1.2.2. Monomer synthesis

The synthesis scheme of (meth)acrylate monomers is shown in Scheme 1-1a and b.

1.2.2.1. 2-Acryloyloxyethyl 9-oxo-9*H*-thioxanthene-3-carboxylate 10,10-dioxide (THA)

Into a 500-ml three-necked flask fitted with a magnetic stirrer, a condenser and a nitrogen inlet, was added 17.30 g (60 mmol) of 9-oxo-9*H*-thioxanthene-3-carboxylic acid 10,10-dioxide, 34.8 g (300 mmol) of 2-hydroxyethyl acrylate, 0.737 g (6.0 mmol) of 4-dimethylaminopyridine, and 290 ml of tetrahydrofuran (THF). After the solution was cooled at 0°C, 13.70 g (66.0 mmol) of dicyclohexylcarbodiimide was added over 15 min. After 1 h of stirring, the reaction vessel was allowed to warm to room temperature, and stirring was continued for an additional 12 h to complete the reaction. The resulting dicyclohexylurea was removed by filtration. After evaporation of THF, residual solid was purified by column chromatography silica gel, chloroform. followed by recrystallization from chloroform / methanol (1:2). Yield 14.1 g 61% ; ^{1}H NMR ($CDCl_3$). δ from TMS: 8.77 (d, 1H, Ar), 8.37 (m, 2H, Ar), 8.31 (dd, 1H, Ar), 8.16 (dd, 1H, Ar), 7.89 (t, 1H, Ar), 7.80 (t, 1H, Ar), 6.45 (dd, 1H, C$\underline{H}_2$=CH–), 6.16 (dd, 1H, CH_2=C$\underline{H}$–), 5.87 (dd, 1H, C$\underline{H}_2$=CH–), 4.66 (m, 2H, CH_2=CHCOOC$\underline{H}_2$$CH_2$ O–), 4.56 (m, 2H, CH_2=CHCOOCH_2C$\underline{H}_2$ O–).

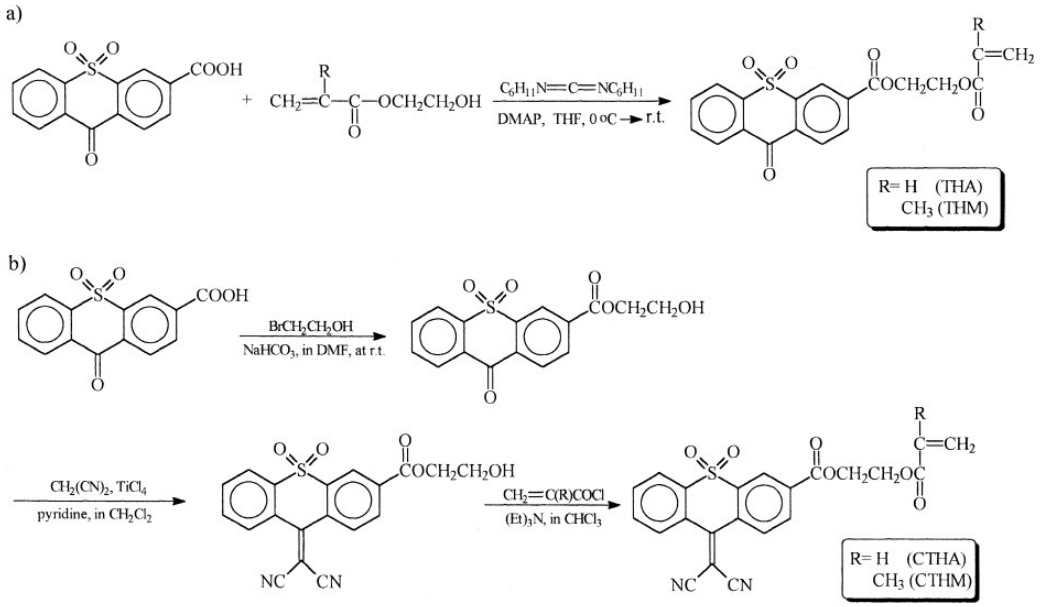

Scheme 1-1

1.2.2.2. 2-Methacryloyloxyethyl 9-oxo-9*H*-thioxanthene-3-carboxylate 10,10-dioxide (THM)

Methacrylate type monomer (THM) was also synthesized in a similar way using 2-hydroxyethyl methacrylate instead of 2-hydroxyethylacrylate. Yield 15.1 g 63% ; ^{1}H NMR ($CDCl_3$) δ from TMS: 8.80 (d, 1H, Ar), 8.39 (m, 2H, Ar), 8.34 (dd, 1H, Ar), 8.20 (dd, 1H, Ar), 7.89 (t, 1H,Ar), 7.80 (t, 1H, Ar), 6.15 (m, 1H, $C\underline{H}_2$=C(CH_3)–), 5.60 (m, 1H, $C\underline{H}_2$=C(CH_3)–), 4.67 (m, 2H, CH_2=C(CH_3)COO$C\underline{H}_2CH_2O$–), 4.54 (m, 2H, CH_2=C(CH_3)COO$CH_2C\underline{H}_2O$–), 1.96 (m, 3H, CH_2=C($C\underline{H}_3$)).

1.2.2.3. 2-Hydroxyethyl 9-oxo-9*H*-thioxanthene-3-carboxylate 10,10-dioxide (TH-OH)

A 200-ml three-necked flask fitted with a magnetic stirrer, a condenser, and a nitrogen inlet was charged with 10.1 g (35 mmol) of 9-oxo-9*H*-thioxanthene-3-carboxylic acid 10,10-dioxide, 3.74 ml (47 mmol) of 2-bromoethanol, 4.41 g (47 mmol) of sodium bicarbonate, and 90 ml of *N,N*-dimethylformamide. The reaction mixture was heated to 85^{o}C for 12 h, and then was poured into 250 ml of distilled water. The organic phase was extracted with chloroform. After the evaporation of chloroform, residual solid was recrystallized from toluene. Yield 9.9 g (85%); ^{1}H NMR ($CDCl_3$) δ from TMS: 8.78 (d, 1H, Ar), 8.36 (m,2H, Ar), 8.31 (dd, 1H, Ar), 8.16 (dd, 1H, Ar), 7.88 (t, 1H,Ar), 7.79 (t, 1H, Ar), 4.54 (m, 2H, –O$C\underline{H}_2CH_2OH$), 4.01 (2m, 2H, –$OCH_2C\underline{H}_2OH$), 2.42 (br, 1H, –O$\underline{H}$).

1.2.2.4. 2-Hydroxyethyl 9-dicyanomethylene-9*H*-thioxathanthene-3-carboxylate 10,10-dioxide (CTH-OH)

Into a 200-ml three-necked flask fitted with a magnetic stirrer, a condenser, a dropping funnel, and a nitrogen inlet was added 4.0 g (12 mmol) of TH-OH, 2.0 g (30 mmol) of malononitrile, and 100 ml of dichloromethane. To the solution was added dropwise 5.6 ml of titanium (IV) chloride over 30 min, and then 14 ml of pyridine at 0^{o}C. The reaction vessel was allowed to warm to room temperature,and stirring was continued for an additional 24 h to complete the reaction. The reaction mixture was poured into 300 ml of water and the organic phase was extracted with dichloromethane. After the evaporation of solvent, residual solid was purified by column chromatography (silica gel, chloroform). Yield 1.7 g (37%) ; ^{1}H NMR ($CDCl_3$) δ from TMS: 8.80 (d, 1H, Ar), 8.38 (dd, 1H, Ar), 8.21 (m, 1H, Ar), 8.13 (d, 1H, Ar), 8.06 (m, 1H, Ar), 7.77 (m, 2H, Ar), 4.53 (t, 2H, –O$C\underline{H}_2CH_2OH$), 3.98 (t, 2H, –$OCH_2C\underline{H}_2OH$), 2.07 (br, 1H, –O$\underline{H}$).

1.2.2.5. 2-Acryloyoxyethyl-9-dicyanomethylene-9*H*-thioxathanthene-3-carboxylate 10,10-dioxide (CTHA)

A 200-ml three-necked flask equipped with a magneticstirrer, a condenser, a dropping funnel, and a nitrogen inlet triethylamine and 100 ml of chloroform and the solution was cooled to 0^{o}C. The mixture of 3.4 ml (41.9 mmol) of acryloyl chloride and 10 ml of chloroform was added dropwise.

After 1 h stirring, the reaction vessel was allowed to warm to room temperature and stirring was continued for 12 h. The reaction mixture was washed with water and dilute sodium bicarbonate solution. After the solvent evaporation, residual solid was purified by column chromatography (silica gel, chloroform) and recrystallization from methanol / chloroform (1/2). Yield 5.2 g (68%); ^{1}H NMR ($CDCl_3$) δ from TMS: 8.81 (d, 1H, Ar), 8.37 (dd, 1H, Ar), 8.23 (m, 1H, Ar), 8.14 (d, 1H, Ar), 8.07 (m,1H, Ar), 7.78 (m, 2H, Ar), 6.44 (dd, 1H, $C\underline{H}_2$=CH–), 6.15 (dd, 1H, CH_2=C$\underline{H}$–), 5.87 (dd, 1H, $C\underline{H}_2$=CH–), 4.64 (m, 2H, CH_2=CHCOOC$\underline{H}_2CH_2$ O–), 4.53 (m, 2H, CH_2=CHCOOC$H_2C\underline{H}_2$ O–).

1.2.2.6. 2-Methacryloyoxyethyl 9-dicyanomethylene-9*H*-thioxathanthene-3-carboxylate 10,10-dioxide (CTHM)

Methacrylate type monomer (CTHM) was synthesized in a similar way using methacryloyl chloride instead ofacryloyl chloride. Yield 5.5 g (65%); ^{1}H NMR ($CDCl_3$) δ from TMS: 8.79 (d, 1H, Ar), 8.37 (dd, 1H, Ar), 8.23 (m,1H, Ar), 8.15 (d, 1H, Ar), 8.08 (m, 1H, Ar), 7.78 (m, 2H, Ar), 6.14 (m, 1H, $C\underline{H}_2$=C(CH_3)–), 5.60 (m, 1H, $C\underline{H}_2$=C(CH_3)–), 4.65 (m, 2H, CH_2=C(CH_3)COOC$\underline{H}_2CH_2$ O–), 4.52 (m, 2H, CH_2=CHCOOC$H_2C\underline{H}_2$ O–), 1.95 (m, 3H, CH_2=C(C$\underline{H}_3$)–).

1.2.3. Polymerization

Polymerization of synthesized monomers was carried out in a glass ampoule under a dry nitrogen atmosphere.2,2'-Azobisisobutyronitrile was used as an initiator. Polymerization conditions are summarized in Table 1-1. The reaction mixture was poured into a large amount of methanol. Recovered polymers were purified 2–3 times by reprecipitation of chloroform or THF solution into acetone,followed by drying in vacuo.

1.2.4. Measurements

NMR spectra were recorded at 50°C with JEOL α-500 spectrometer operating at 500 MHz for ^{1}H and 125 MHz for ^{13}C. UV spectra were obtained in THF solutions using a JASCO V-500 UV/vis/NIR spectrometer. The molecular weight of synthesized polymers were estimated by gel

Table 1-1 Polymerization conditions and characteristics of polymers

Monomer	Solvent	Concentration (mol/l)	Temperature (°C)	Time (h)	Yield (%)	Mn ($\times 10^4$)	Mw ($\times 10^4$)
THA	Benzene	0.5	70	24	59	2.9	9.6
	Toluene	0.5	70	24	52	1.8	4.2
	THF	1.0	70	24	15	1.1	1.7
	DMF	1.0	70	24	55	1.2	2.5
	DMF	1.0	60	48	60	1.6	4.1
THM	Benzene	0.3	70	24	82	1.8	6.0
	THF	1.0	70	24	82	2.7	11.4
CTHA	DMF	1.0	60	48	33	0.6	1.6
CTHM	DMF	1.0	60	8	80	$>50^a$	$>50^a$

AIBN (1 mol% of monomer) was used as an initiator.
[a]Average molecular weight is higher than the exclusion limit of the GPC column.

permeation chromatography using a column packed with styrene–divinylbenzene gel beads. THF was used as an eluent and the molecular weight was calibrated using polystyrene standards (Shodex). Glass transition temperature (T_g) was determined from differential scanning calorimetry (DSC) chart recorded by SEIKO Instruments DSC 220 under nitrogen at heating rate of 10°Crmin. Redox potentials were measured with cyclic voltammetry in a one-compartment cell with a polarization unit (TOHO PS-06) The measurements were conducted for the cast films on platinum working electrode in dry acetonitrile containing tetrabutylammonium perchlorate (0.1 M) as an electrolyte under a nitrogen atmosphere. Platinum spiral was used as a counter electrode, and Ag/AgCl as a reference electrode.

Samples for drift mobility measurements were prepared as follows. Titanyl phthalocyanin (TiOPC) was spin coated from organic solvent onto aluminum vapor-deposited on a glass slide, then dried at 90°C for 30 min. A polymer solution in 1,2-dichloroethane or DMF (0.15 g/ml) was filtered through a 0.5-μm filter, followed by spreading on TiOPC layer (<0.2 μm) using a wire bar coater. The film was allowed to dry for several hours at room temperature and then dried at 90°C for 1 h to remove residual solvent (for DMF solution, it was additionally dried in vacuo at 90°C for 2 h). Semitransparent gold electrode was prepared on the film surface by vacuum deposition at a pressure of 10^{-5} Torr. Film thickness was determined by a profilometer (DEKTAK II, Solan). Electron drift mobility was measured with a conventional time-of-flight method at room temperature using a xenon flash lamp (Hamamatsu photonics, L2359) and digitizing oscilloscope (GOULD, DSO630). Photoinduced surface potential discharge (PID) curves were recorded using an electrostatic paper analyzer (Kawaguchi Electric Works, Model EPA-8100) irradiating white light with an intensity of 8.2 lx.

1.3. Results and discussion

When benzene was used as a solvent to polymerize THA and THM, the produced polymer was precipitated from the reaction mixture. In the case of a polar solvent such as THF or dimethylformamide (DMF), polymerization proceeded in a homogeneous system. CTHA and CTHM were polymerized in DMF. Methacrylate type monomers (THM and CTHM) provided higher molecular weight polymers in higher yields than acrylate type monomers.

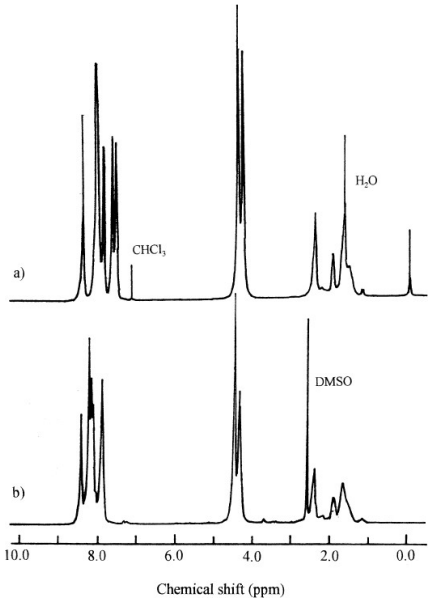

Fig. 1-1 ^{1}H NMR spectra of poly(THA) (a) and poly(CTHA)(b) measured at 50°C and 500 MHz in $CDCl_3$ and DMSO-d_6 solutions, respectively.

Structures of polymers were identified by ^{1}H NMR. Fig. 1-1 shows ^{1}H NMR spectra of poly(THA) and poly(CTHA). Signals resonated between 1.4 and 2.0 ppm were assigned to the main chain methylene protons, those that appeared in the region of 2.2 to 2.6 to the main chain methine protons. Signals around 4.5 ppm were assigned to the two types of methylene proton in the side chain ethylene unit. Aromatic protons appeared in the range of 7.6 to 8.7 ppm. The relative intensities of these signals were almost equal to the expected values from the polymer structure. ^{1}H NMR spectra of poly(THM) and poly(CTHM) were almost equal to those of poly(THA) and poly(CTHA) except that the α-methyl proton signals, which exhibited triplet splitting due to the tacticity, appeared around 1 ppm in the absence of methine proton signal around 2.4 ppm.

All the polymers were colorless and soluble in polar solvents such as THF, DMF and DMSO. UV spectra of the polymers were observed in a THF solution. The results were summarized in Table 1-2. Poly(THA) and poly(THM) had two absorption maxima at 272 and 288 nm, while poly(CTHA) and poly(CTHM) had absorption maximum at 312 nm. These absorptions were almost identical to those corresponding low-molecular-weight compounds.

The chloroform or THF solution of polymer was cast on a platinum electrode and the cyclic voltammograms were recorded in acetonitrile containing 0.1 M (n-Bu)$_4$ NClO$_4$. Fig. 1-2 shows the cyclic voltammogram of a cast film of poly(THA). The polymer had two pairs of redox peaks, which were symmetrical and well-defined. The other polymers also had two pairs of redox peaks as shown in Table 1-2. Poly(THA) and poly(THM) had the first and the second reduction peaks around -0.88 and -1.36 V vs. Ag/AgCl, while poly (CTHA) and poly (CTHM) had reduction peaks around -0.53 and -0.86 V. Thus the latter polymers were more easily reduced than the former, which indicates that the dicyanomethylene group has stronger electron withdrawing effect than carbonyl group. The polymers showed reversible electrochromism, with the color change from colorless (neutral state) to deep green (reduction state).

The electron mobility of the polymers was determined by the time-of-flight method. The mobility, m, was calculated according to the following equation:

$$\mu = L^2 / t_T V$$

where L is the sample thickness, t_T the transit time, and V the applied voltage. The methacrylate type polymers were

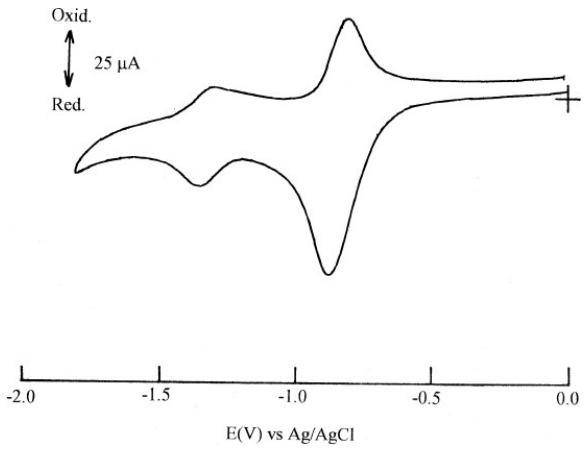

Fig. 1-2 Cyclic voltammogram of a cast film of poly THA. measured inacetonitrile with 0.1 M (n-Bu)$_4$NClO$_4$; scanning rate 150 mV/s.

Table 1-2 Properties of synthesized polymers

Polymer	$\lambda_{max}1$[a] (nm)	$\lambda_{max}2$[a] (nm)	Cut off[a] (nm)	T_g[b] (°C)	Redox potential (V)[c]			
					Epc^1	Epc^2	Epa^1	Epa^2
P(THA)	271	288	335	115	−0.87	−1.35	−0.80	−1.29
P(THM)	273	288	330	125	−0.89	−1.37	−0.80	−1.29
P(CTHA)	311	–	364	163	−0.52	−0.85	−0.37	−0.78
P(CTHA)	312	–	364	172	−0.54	−0.86	−0.37	−0.80

[a]UV spectra were measured in THF solution.
[b]Glass transition temperature measured by DSC.
[c]Redox potentials (vs. Ag/AgCl) were measured in CH_3CN containing $(n\text{-Bu})_4NClO_4$.

too brittle to provide a good film with enough thickness, although they had higher average molecular weight than the acrylate type polymers. The brittleness of the methacrylate type polymers may be attributed to the α–methyl group, which hinders the main chain rotation. Therefore, only the charge mobility of acrylate type polymers was determined. Fig. 1-3 shows the mobility of the polymers plotted against the square root of the electric field. A good linear relation was observed between the mobility and the square root of the electric field for both polymers. As a comparison, the mobility of a low molecular weight model compound *n*-butyl ester of thioxanthene derivative. doped in poly(methyl methacryalate) was shown. The butyl ester could be dissolved only up to 40wt.%. The mobility of composite doped with the model compound was lower than that of polymer by a factor of 100. This difference can be explained by the concentration difference of the thioxanthene units: 40 wt.% for the molecularly dispersed system vs. 63 wt.% for the polymer.

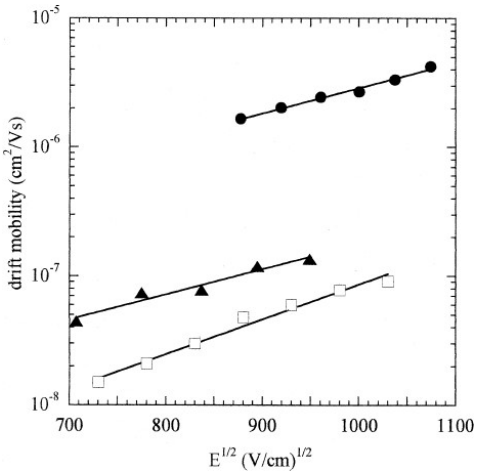

Fig. 1-3 Field dependence of drift mobility (●) poly (THA), (▲)poly(CTHA), (□) PMMA doped with 40 wt.% of n-butyl 9-oxo-9*H*-thioxanthene-3-carboxylate 10,10-dioxide.

It is noteworthy that poly(CTHA) had lower mobility than poly(THA), although the former had lower reduction potentials. In order to examine the difference, molecular orbital calculations by PM3 method were carried out with MOPAC Ver.6 using *n*-butyl ester of thioxanthene derivatives as model compounds. It is believed that the electron transport process is governed by the hopping process involving the radical anion. Therefore, the structural evaluation of the lowest unoccupied molecular orbital (LUMO) makes it possible to explain the difference of mobility. In the case of HTM, it is proposed that the important factor for high hole drift mobility is a well-balanced positive charge

distribution in highest occupied molecular orbital in an HT molecule[13]. Fig. 1-4 shows the electron density maps of LUMO for both molecules. In the case of dicyanomethylated thioxanthene (Fig. 1-4b), electrons are rather localized around the dicyanomethyl group, while the unmodified one with carbonyl group (Fig. 1-4a) has a well-balanced electron distribution. This is considered to be the main reason for higher drift mobility.

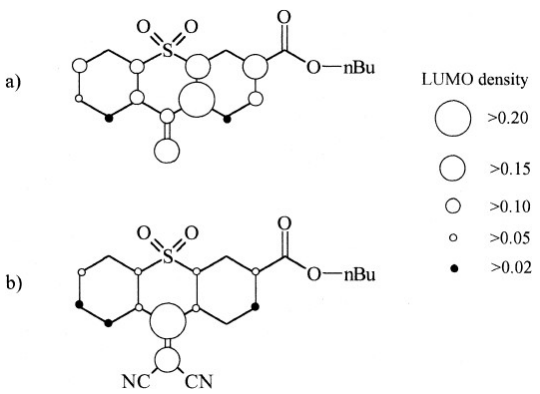

Fig. 1-4 LUMO density maps of n-butyl ester of thioxanthene derivatives. (a) Unmodified, (b) dicyanomethylated

The organic photoconductor device was prepared to measure the photoinduced surface potential discharge (PID) curve. The photoconductor device consisted of aluminum as a substrate, titanyl phthalocyanine as a charge generation layer (CGL; 0.3 μm), poly(THA) as the charge transport layer (CTL; 3 μm). The resulting PID curve is shown in Fig. 1-5. When a corona charge of 6 kV was given to the polymer film the surface potentials increased to 221 V in 5 s. After the corona charging was stopped, the surface potential gradually decreased by 27% in 5 s. These results indicate the stable character of the film. As the film was exposed to white light, the surface potential immediately decreased in less than 1 s and stayed almost constant at 49 V residual potential. after 10 s. The half-decay exposure was determined to be 0.59lx s. This value is close to those of organic photoconductors used commercially, which indicates that poly(THA) could be applied for practical use when the residual surface potential is properly controlled.

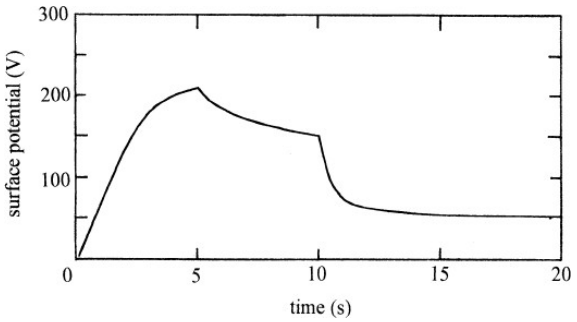

Fig. 1-5 Photoinduced surface potential discharge curve obtained for poly(THA) film. 5 s; the stop of corona charge 6 kV., 10 s; the start of exposure of white light 8.2 lx.

1.4. Conclusion

Novel electron transporting polymers were prepared from acrylate or methacrylate having thioxanthene derivative. Resulting polymers were soluble in common organic solvents such as THF and DMF, and showed electrochemical activity. Drift mobility measurements and molecular orbital calculations revealed that well-balanced electron distribution in LUMO in electron transporting

molecule plays an important role for high electron drift mobility. Photoinduced surface potential discharge curve showed that prepared polymers can be applied to organic photoconductor device.

References

1) R.O. Loutfy, B.S. Ong, *Can. J. Chem*. **62** (1987) 2546.

2) E. Han, L. Do, Y. Niidome, M. Fujihira, *Chem. Lett*. (1994). 969.

3) W.D. Gill, *J. Appl. Phys.* **43** (1972) 5033.

4) P.M. Borsenberger, T.-M. Kung, W.B. Vreeland, *J. Appl. Phys.* **68** (1990) 4100.

5) H. Tokuhira, M. Era, T. Tsutsui, S. Saito, *Appl. Phys. Lett*. **66** (1995). 3433.

6) J. Bettenhausen, P. Strohriegl, W. Bru¨tting, H. Tokuhisa, T. Tsutsui, *J. Appl. Phys.* **82** (1997) 4957.

7) P.M. Borsenberger, W.T. Gruenbaum, *J. Polym. Sci., Part B* **34** (1996). 575.

8) K. Nagasawa, Y. Akao, M. Tanabe, Y. Yamada, *Polym. Prepr. Japan*. **41** (1992) 851.

9) J.H. Shim, K. Ogino, H. Sato, *Synth. Met.* **69** (1995) 575.

10) J.H. Shim, K. Ogino, H. Sato, Y. Pei, *J. Imag. Sci. Technol*. **40** (1996) 164.

11) J.M. Son, Y. Sakaki, K. Ogino, H. Sato, *IEEE Trans. Electron Devices* **44** (1997). 1307.

12) K. Ogino, T. Nomura, T. Shichi, S-H. Park, H. Sato, T. Aoyama, T. Wada, *Chem. Mater.* **9** (1997) 2768.

13) T. Kitamura, M. Yokoyama, *J. Appl. Phys*. **69** (1991) 821.

Chapter 3 Polymers Having Hole and Electron Transport Units by Friedel–Crafts Reaction

Abstract: Polymers having 2,5-diphenyl-1,3,4-oxadiazole (BCO) or anthracene (BCA) as an electron transport unit and *N,N*'-diphenyl-*N,N*'-bis(4-butylphenyl)-benzidine (BTPD) as a hole transport unit were prepared by condensation polymerization using Friedel–Crafts reaction. It was found that BCO was less reactive than BCA. The low reactivity of the BCO monomer can be explained by the oxygen atom in the oxadiazole unit, which acts as a Lewis base and reduces the activity of the catalyst. The redox behavior measured by cyclic voltammetry showed for both BTPD-BCO and BTPD-BCA almost the same oxidation potential. In addition, the BTPD-BCO also exhibited a reduction peak. Hole and electron drifts mobility of the polymers were measured by the time-of-flight method. The hole drift mobility of both BTPD-BCO and BTPD-BCA was 7.4×10^{-5} cm^2 V^{-1} s^{-1}. The electron drift mobilities of BTPD-BCO and BTPDBCA were 6.5×10^{-5} cm^2 V^{-1} s^{-1} and 5.2×10^{-6} cm^2 V^{-1} s^{-1}, respectively.

3.1. Introduction

Organic charge transport materials play an important role in many electrical and optical applications such as organic photoconductors and electroluminescence (EL) devices. Many of the organic charge transport materials have been investigated by a number of researchers.[1–7] However, in most of the organic charge transport materials, the electrical current is dominated by hole transport capacity. It is obvious that efficiency of the electrical and optical applications would require a good balance of hole and electron transport capacity in the device. It is reported that a balance of the rate of transport of holes and electrons in the device is important in achieving high efficiency for EL devices.[8] Previously the research group the author belonged to have studied the condensation polymerization of triphenylamine (TPA) derivatives with anthracene derivatives.[9] TPA derivatives are one of the most widely used hole-transport materials (HTM) due to their high hole mobility. It was assumed that anthracene unit would help to transport electrons, because of its electron-rich structure and low electronic band gap.[10] While this novel polymer showed excellent hole transport ability, its electron transport ability was poor.

In this chapter, polymers containing 2,5-diphenyl-1,3,4-oxadiazole or anthracene unit and *N,N'*-diphenyl-*N,N'*-bis(4-butylphenyl)-benzidine (BTPD) unit were prepared, since oxadiazole or anthracene derivatives are known to have high electron mobility.[11,12] The electron and hole mobilities of the resulting polymer were compared.

3.2. EXPERIMENTAL

3.2.1 General

All the reagents for the synthesis were commercially obtained and were used without further purification unless otherwise noted. The chlorobenzene was distilled over calcium hydride and used

as a solvent for polymerization.

3.2.2 *N,N'*-Diphenyl-*N,N'*-bis(4-butylphenyl)benzidine

N,N'-Diphenyl-*N,N'*-bis(4-butylphenyl)benzidine (BTPD) was synthesized from *N,N'*-diphenylbenzidine and 4-bromo-4-*n*-butylbenzene by the Tosoh method (Scheme 3-1). Into a 300-mL flask, 5.7 g (0.0168 mol) of *N,N'*-diphenylbenzidine, 12.5 g (0.042 mol) of 1-bromo-4-*n*-butylbenzene, 4.74 g (0.0504 mol) of sodium *tert*-butoxide, 0.00235 g (0.0105 mmol) of palladium acetate, 0.03 mL (0.042 mmol) of tri(*tert*-butyl)phosphine (1.0 M xylene solution), and 50 mL of xylene were added. The reaction mixture was stirred at 120°C until the disappearance of the *N,N'*-diphenylbenzidine, as verified by TLC. After cooling, the reaction mixture was washed with water. The oil layer containing BTPD was concentrated and purified by column chromatography (toluene: hexane = 1:3). BTPD was obtained in 78% yield.

^{1}H NMR ($CDCl_3$) δ from TMS: 0.95, 1.35, 1.60 and 2.60 ppm [6H; -CH_3, 4H; -CH_2, 4H; -CH_2, 4H; -CH_2] and 6.95–7.45 ppm [26H; aromatic protons].

Scheme 3-1

3.2.3 2,5-Bis[4-(chloromethyl)phenyl]-1,3,4-oxadiazole

To a three-necked 200-mL flask equipped with a magnetic stirrer were added p-chloromethyl benzoic acid (8.5 g, 0.0498 mol) and 40 mL of thionyl chloride. The reaction mixture was stirred under reflux until the disappearance of the *p*-(chloromethyl) benzoic acid, as verified by TLC. After 4.5 h, excess amount of thionyl chloride were distilled away to obtain 4-chloromethylbenzoyl chloride. 1-Methyl-2-pyrrolidone (NMP) (25 mL) was added dropwise to the product. After cooling to 0°C, 1.22 mL (0.025 mol) of hydrazine monohydrate in 15 mL of NMP was slowly added to this solution while stirring at the reaction temperature below 0°C. The reaction mixture was warmed to room temperature in 0.5 h and was stirred at room temperature for 0.5 h. Water was poured in the reaction mixture and the product was washed with water. The washed product was filtrated and dried in vacuum. After drying, the product was recrystallized from methanol solution to obtain 1,2-bis[4-(chloromethyl)phenyl]hydrazine in 31% yield.

To a three-necked 200-mL flask equipped with a magnetic stirrer were added 5.1 g (0.0151

mol) of 1,2-bis[4-(chloromethyl)phenyl]hydrazine and 70 mL of thionyl chloride. The reaction mixture was stirred under reflux until the disappearance of the 1.2-bis[4-(chloromethyl)phenyl]-hydrazine, as verified by TLC. After 2 h, excess amount of thionyl chloride were distilled away. The product was recrystallized from methanol solution. BCO was obtained with a yield of 78% (Scheme3-2).

^{1}H NMR ($CDCl_3$) δ from TMS: 4.70 ppm [4H; -CH_2Cl] and 7.50 and 8.10 ppm [8H; aromatic protons].

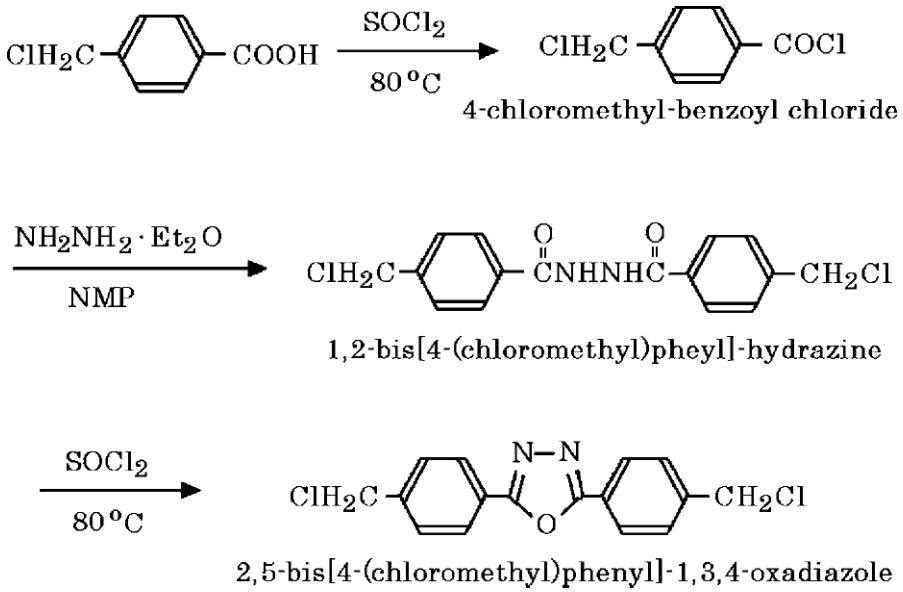

Scheme 3-2

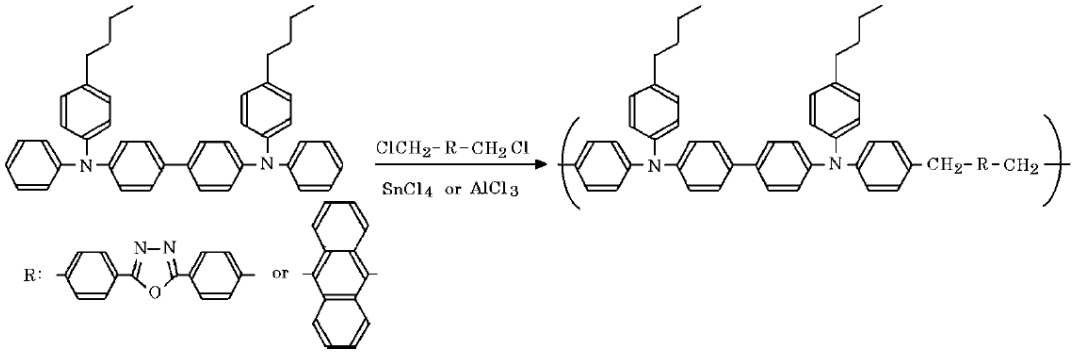

Scheme 3-3

3.2.4 Polymerization

The polymerization was carried out under nitrogen atmosphere using chlorobenzene as a solvent. Tin(IV) chloride and aluminum(III) chloride were used as catalysts (Scheme 3-3). Polymer

was recovered by pouring the reaction mixture into excess amount of methanol and then purified by reprecipitation with pouring the toluene solution into acetone, followed by drying in vacuum.

3.2.5 Measurement

The proton nuclear magnetic resonance (^{1}H NMR) measurements were conducted at 30^{o}C with JEOL α−500 spectrometer operating at 500 MHz in $CDCl_3$ or dimethylsulfoxide (d6) and with tetramethylsilane (TMS) as an internal standard. Molecular weights of the polymers were estimated by gel permeation chromatography (GPC) using JASCO 880-PU pump, a column packed with styrene–divinylbenzene gel beads, and a JASCO UV-970 detector. Chloroform was used as an eluent, and the molecular weight was calibrated using polystyrene standards (Shodex). UV–vis absorption spectra were obtained by a JASCO Ubest-30 UV-Vis spectrometer. Photoluminescence (PL) spectra were measured using JASCO FT-6500 spectrofluorometer. The measurements of UV–vis and PL spectra were carried out in a toluene solution or as a film. The redox potential was measured with cyclic voltammetry in a one-compartment cell with a polarization unit (TOHO PS-06). The measurement was conducted for a film cast on a carbon working electrode in dry acetonitrile containing 0.1 M tetra-*n*-butylammonium perchlorate (Bu_4NClO_4) as electrolyte under nitrogen atmosphere at the scanning rate of 20 mV/s. Platinum spiral was used as a counter electrode and Ag/AgCl as a reference electrode. Samples for the drift mobility measurements were prepared as follows. Titanyl phthalocyanine (TiOPc) was spin-coated from a suspension in an organic solvent onto aluminum deposited on a slide glass. The toluene solution (typically 0.5 g/mL) of the polymer was filtered through a 0.5-μm filter. The polymer solution was then spread over the TiOPc layer using a wire bar. The films were dried at 90^{o}C for 1 h to remove residual solvent. A semitransparent gold electrode was prepared on the film surface by vacuum deposition at the pressure of 3–7 × 10^{-6} Pa. The thickness of this film was determined by a profilometer (Dektak II, Solan). Drift mobility was measured with a conventional time-of-flightmethod at room temperature using xenon flash lamp (Hamamatsu Photonics, L2359), and digitizing oscilloscope (Gould, DSO 630).

3.3. RESULTS AND DISCUSSION

3.3.1 Polymerization

The polymers were synthesized by condensation polymerization using Friedel–Crafts reaction of alkyl-TPD and dihalide (Scheme 3-3). Table 3-1 shows the results of polymerization of butyl-TPD (BTPD) with 2,5-bis(4-chloromethylphenyl)-1,3,4-oxadiazole (BCO) and bis(chloromethyl)anthracene (BCA). Polymerization with BTPD and BCA gave a polymer in 96% yield and M_n of 9.8×10^3 in the presence of 4.0 mol % of the $SnCl_4$ catalyst. Using $AlCl_3$ as a catalyst, the M_n and yield were almost the same as for the polymer prepared using $SnCl_4$ as a catalyst. On the other hand, polymerization of BTPD with BCO was unsuccessful at the same reaction conditions as

those of BTPD with BCA. It was necessary to use no less than 150 mol % of the catalyst to react efficiently BTPD with BCO. Polymerization between BTPD and BCO units gave a product with 95% yield and M_n of 7.5×10^3 in the presence of 200 mol % of catalyst after 24 h. Using $AlCl_3$ as a catalyst, under the same conditions, a polymer having M_n of 5.0×10^3 was obtained with the yield of 63%. The low reactivity of BCO can be attributed to the presence of the oxygen atom in the oxazole unit, which acts as Lewis base and reduces the activity of the catalyst.

Table 3-1 Reaction Conditions and Molecular Weight of Polymers

Halides[a]	Catalyst	Catalyst (mol %)	Time (h)	Yield (%)[b]	M_n (10^3)	M_w (10^3)
BCO	$SnCl_4$	200	24	95 (38)	7.5	13.1
BCO	$SnCl_4$	150	24	91 (33)	7.5	12.1
BCO	$SnCl_4$	100	24	56 (11)	1.8	4.3
BCO	$SnCl_4$	4	24	0	–	–
BCO	$AlCl_3$	200	24	63	5	9
BCO	$AlCl_3$	4	24	0	–	–
BCA	$SnCl_4$	4	1.5	96	9.8	10
BCA	$AlCl_3$	4	1.5	97	10	12

[a] Amine = halide = 1 mmol.
[b] The value in parentheses is the yield of insoluble parts of polymer.

3.3.2 Polymer Structures

Figure 3-1 shows ^1H NMR spectra of the polymers containing the BCO and BCA units. Both polymers showed two signals from methylene groups (-CH_2-): BTPD-BCO at 4.0 and 3.8 ppm, and BTPD-BCA at 5.0 and 4.6 ppm. The signals resonating at lower magnetic fields were assigned to a methylene group at the para-position of the phenyl ring, while the signals at higher magnetic fields were assigned to methylene protons linked with the *meta*-position of the butyl phenyl group. The signals were assigned by considering the NMR spectra of polymers synthesized with methyl-TPD (MTPD) and paraformaldehyde by using condensation polymerization.[13] The intensity ratio of the signals of the *para*- and *meta*-positions for BTPD-BCO was 1.0:1.0, and that for BTPD-BCA was 1.0:0.3. The lower *meta*-position ratio for the BCA polymer can be explained by the steric hindrance: larger anthracene units prevent the methylene carbonium ion to attack at the *meta*-position of butyl group.[9] The reaction at the *meta*-position of butylphenyl unit indicates that the BTPD monomer is tetra- or hexa-functional monomer. The insoluble polymer was produced for BTPD-BCO polymer, which had high *meta* ratio.

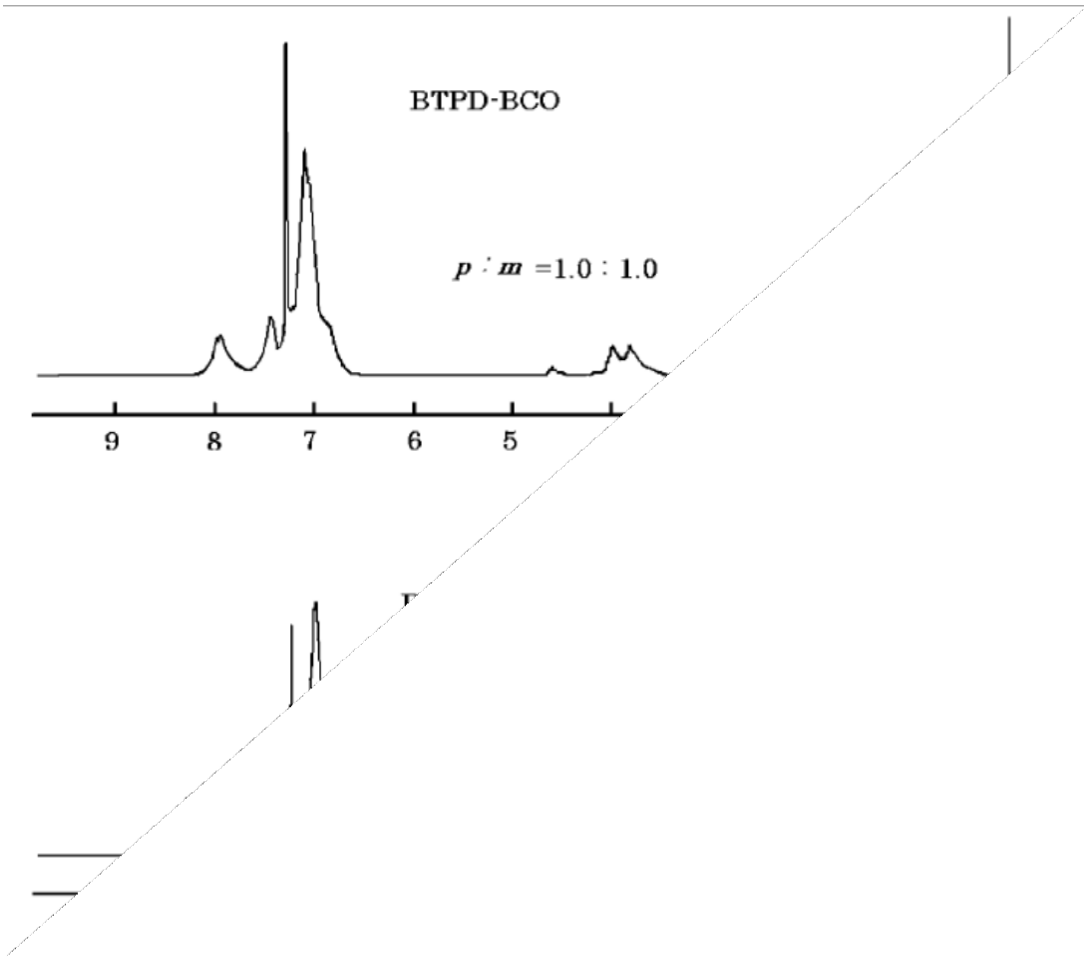

Fig. 3-1 ^{1}H NMR spectra of polymers.

3.3.4 Optical and Electrochemical Properties

The UV–vis absorption spectra of the BTPD-BCO and BTPD-BCA are shown in Fig. 3-2. The BTPD-BCO polymer exhibited peaks at 300 and 365 nm, and BTPD-BCA peaks at 311 and 356 nm. The onset of the absorptions leads to the band-gaps for BTPD-BCO and BTPD-BCA of 3.07 and 3.03 eV, respectively. The photoluminescence (PL) emission spectra of the BTPD-BCO and BTPD-

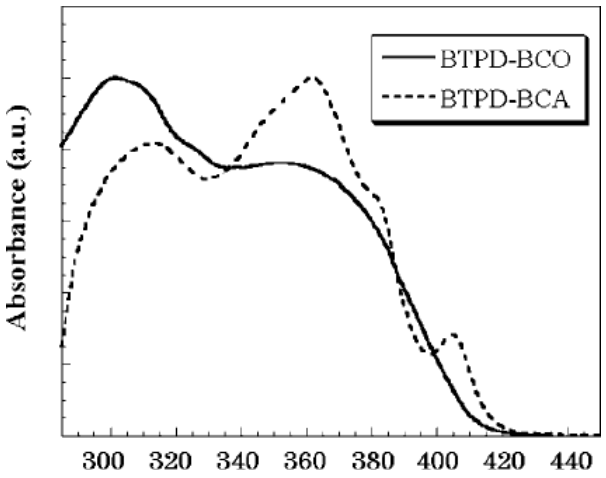

Fig.3-2. UV–vis spectra of polymers

BCA are shown in Fig.3-3, maxima at 440 and 478 nm, respectively. Fig. 3-4 shows oxidation–reduction curves of the polymers. Both polymers showed anodic peak of oxidation at 1.02 eV and reduction at 0.5 eV. The peaks appearing at positive voltage are attributed to the oxidation potentials of the BTPD units. The BTPD-BCO showed also one peak at negative voltage. It can be assumed that introduction of the BCO unit improves electron-withdrawing ability of the polymer. On the other hand, the BTPD-BCA polymer showed no peak on the negative voltage side. It is noteworthy that both polymers had the same oxidation potential at positive side, which indicates that there were no effects of the introduction of the electron transport moiety on the oxidation potentials of the polymers. The HOMO and LUMO energy levels of the BTPD-BCO obtained from CV and UV–vis spectrum were 5.92 and 2.85 eV. The HOMO and LUMO energy levels of the BTPD-BCA were 5.92 and 2.89 eV.

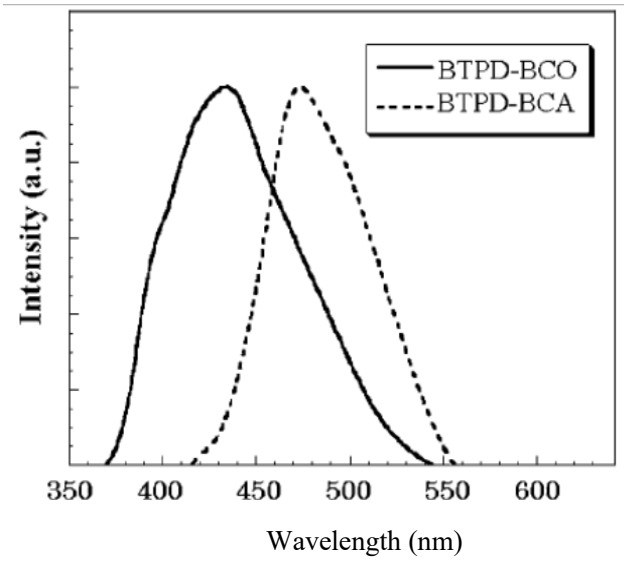

Fig. 3-3. PL spectra of polymers

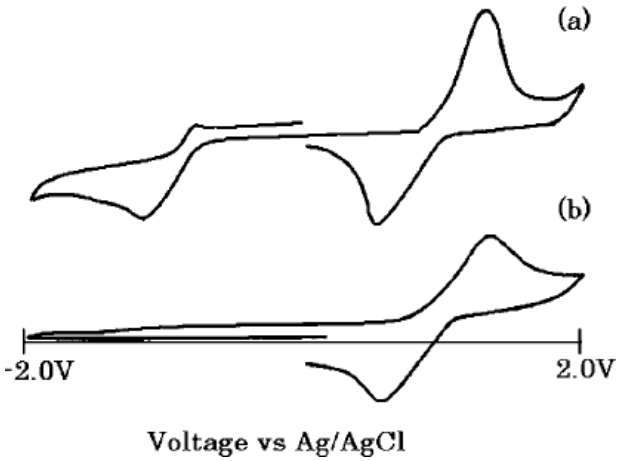

Fig. 3-4. Cyclic voltammograms of polymers: (a) BTPD-BCO; (b) BTPD-BCA.

BTPD-BCO and BTPD-BCA had glass-transition temperatures (T_g) of 159°C and 195°C, respectively. The higher T_g of BTPD-BCA polymer can be attributed to the bulkiness of anthracene unit, which suppress the mobility of the polymer chain.

3.3.5 Time-of-Flight (Charge Mobilities)

The hole and electron drift mobility were measured by the standard time-of-flight method. The hole (μ_h) and electron mobilities (μ_e) were calculated according to the following equation:

$$\mu = L^2 / t_T V$$

where L is the sample thickness, t_T is the transit time, and V is the applied voltage. The t_T is determined from the transit time determined by the double logarithmic plots of current i versus time t. Table 3-2 compares the mobilities of holes and electrons and their balance values at the applied voltage of 1.3×10^5 V/cm. According to the values given in the Table 3-2, the BTPD-BCO polymer had the charge balance μ_h / μ_e of 1.14, while the BTPDBCA polymer charge balance was 14.1. The charge balance value for BTPD-BCO of 1.14 is close to the ideal value of 1. Hole drift mobility of both BTPD-BCO and BTPD-BCA at an applied field of 1.3×10^5 V/cm was 7.4×10^{-5} cm^2 $V^{-1}s^{-1}$. In previous reports, the mobilities of holes in the BTPD-aldehyde polymer were on the order of 10^{-5} cm^2 V^{-1} s^{-1} regardless of the applied voltage.[14] Therefore, the electron transport unit showed negligible effect on the hole transport ability. Electron transport of the BTPD-BCO polymer was 14 times higher than that of the BTPD-BCA polymer. Electron transport mobility of the polymer films containing oxadiazole unit was reported in the order of 10^{-4}–10^{-6} cm^2 $V^{-1}s^{-1}$.[15,16] This value is almost the same as this experiment.

Table 2. Hole (μ_h) and Electron Mobilities (μ_e) of BuTPD-BCA and BuTPD-BCO at an Applied Field of 1.3×10^5 V/cm.

	Mobility μ_h (10^{-5}) (cm^2 V^{-1} s^{-1})	Mobility μ_e (cm^2 V^{-1} s^{-1})	μ_h/μ_e
BTPD-BCA	7.3	5.2×10^{-6}	14.1
BTPD-BCO	7.4	6.5×10^{-5}	1.14

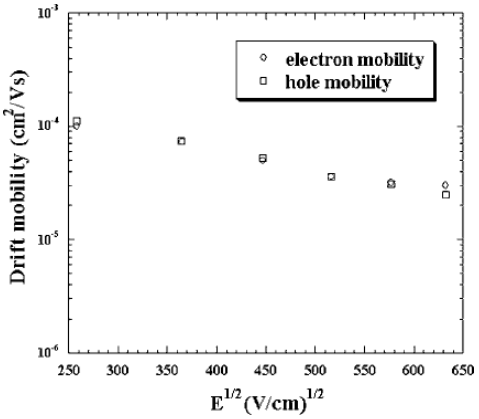

Fig. 3-5. Drifts mobility against the square root of applied field E(V/L) for BTPD-BCO. Circles: hole mobility; squares: electron mobility.

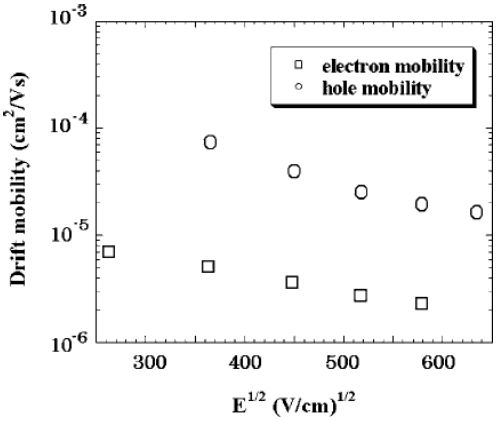

Fig. 3-6. Drifts mobility against the square root of applied field E(V/L) for BTPD-BCA. Circles: hole mobility; squares: electron mobility.

Figures 3-5 and 3-6 showing the plots of log l versus $E^{1/2}$ indicate linear relationships with negative slopes. This negative slope has also been observed in other polymers[13,15,17–19] and has been attributed to the presence of trap sites in the polymer film.[15]

3.4. CONCLUSIONS

Polymers containing TPD and oxadiazole or anthracene units were prepared by Friedel–Crafts reaction. Polymerization between BTPD and BCA units occurred in the presence of 4.0 mol % of catalyst. On the other hand, it was necessary to use more than 150 mol % of catalyst to react BTPD with BCO. The low reactivity of BCO polymer was explained by the presence of oxygen atom in oxadiazole unit, which reacts as a base
and reduces the catalytic activity. The polymerization occurred not only at the *para*-position of the phenyl group but also at the *meta*-position of the butylphenyl group. From the results of CV, the BTPD-BCO showed not only the oxidation but also a reduction peak. It can be assumed that introduction of the BCO improved the electron withdrawing ability of the polymer. The hole and electron drift mobility were measured by the standard time-of-flight method. BTPD-BCO showed an excellent charge balance, and the electron mobility of the BTPD-BCO was 14 times higher than that of BTPD-BCA.

REFERENCES AND NOTES

1) Gill, W. D. *J Appl Phys* **1972**, *43*, 5033.

2) Burrows, P. E.; Gu, G.; Bulovic, V.; Shen, Z.; Forrest, S. R.; Thompson, M. E. *IEEE Trans Electron Devices* **1997**, *44*, 1188.

3) Aratani, S.; Kawanishi, T.; Kakuta, A. *Jpn J Appl Phys* **1996**, *35*, 2184.

4) Thelakkat, M. *Macromol Mater Eng* **2002**, *287*, 442.

5) Wang, X.; Chen, Z.; Ogino, K.; Sato, H.; Strzelec, K.; Miyata, S.; Luo, Y.; Tan, H. *Macromol Chem Phys* **2002**, *203*, 739.

6) Zhou, X.; Blochwitz, J.; Pfeiffer, M.; Nollau, A.; Fritz, T.; Leo, K. *Adv Funct Mater* **2001**, *11*, 310.

7) He, Q.; Lin, H.; Weng, Y.; Zhang, B.; Wang, Z.; Lei, G.; Wang, L.; Qiu, Y.; Bai, F. *Adv Funct Mater* **2006**, *16*, 1343.

8) Cha, S. W.; Joo, S. H.; Jeong, M. Y.; Jin, J. I. *Synth Met* **2005**, *150*, 309.

9) Mori, T.; Strzelec, K.; Sato, H. *Synth Met* **2002**, *126*, 165.

10) Ha, J.; Vacha, M.; Khanchaitit, P.; Ath-Ong, D.; Lee, S. H.; Ogino, K.; Sato, H. *Synth Met* **2004**, *144*, 151.

11) Hamada, Y.; Adachi, C.; Tsutsui, T.; Saito, S. *Jpn J Appl Phys* **1992**, *31*, 1812.

12) Jin, S. H.; Kim, M. Y.; Kim, J. Y.; Lee, K.; Gal, Y. S. *J Am Chem Soc* **2004**, *126*, 2474.

13) Son, J. M.; Ogino, K.; Yonezawa, N.; Sato, H. *Synth Met* **1998**, *98*, 71.

14) Takahashi, C.; Moriya, S.; Fugono, N.; Lee, H. C.; Sato, H. *Synth Met* **2002**, *129*, 123.

15) Kolb, E. S.; Gaudiana, R. A.; Mehta, P. G. *Macromolecules* **1996,** *29*, 2359.

16) Son, J. M.; Nakao, M.; Ogino, K.; Sato, H. *Macromol Chem Phys* **1999**, *200*, 65.

17) Stewart, J. J. P. J *Comput Chem* **1989**, *10*, 221.

18) Chen, B.; Liu, Y.; Lee, C. S.; Yu, G.; Lee, S. T.; Li, H.; Gambling, W. A.; Zhu, D.; Tian, H.; Zhu, W. *Thin Solid Films* **2000**, *363*, 173.

19) Lee, H. M.; Oh, D. K.; Lee, C. H.; Lee, C. E.; Lee, D. W.; Jin, J. I. *Synth Met* **2001**, *119*, 473.

Chapter 4 Novel Electroluminescent Polymer based on Phenoxazine and Fluorene Derivatives

Abstract: A new electroluminescent polymer was prepared by oxidative coupling copolymerization of *N*-(4-*n*-butylphenyl)phenoxazine (PPX) and 9,9-di-*n*-butylfluorene (DBF) using iron (III) chloride. The obtained polymers were soluble in common organic solvents and had number-average molecular weight as high as 10,000. The UV–vis absorption maximum and photoluminescence peak shifted to longer wavelengths with the increase of PPX content. The increase of PPX content also caused increase of hole mobility and decrease of electron mobility. A simple single-layer light-emitting-diode device having a structure of indium tin oxide/polymer/Ca/Al was fabricated. The polymer containing 30% of PPX unit showed highest electroluminescent properties with a maximum luminance of 1084 cd/m^2 at 15.5 V operating voltage.

4.1. Introduction

Considerable progress has been made since Burroughes et al. found that electroluminecent (EL) device can be fabricated using a conjugated polymer, poly(*para*-phenylene vinylene), in 1990[1]. An optimized EL device requires balanced hole and electron injections from both electrodes and comparable charge transporting properties for both charge carriers Thus, synthesis of novel electron-transporting EL polymers is needed to improve the device performance. Poly(p-phenylenecyanovinylene) (CN-PPV)[2] and its derivatives are well known electron-transporting EL polymers. The introduction of electrondeficient oxadiazole ring as side or main chain has also proved to increase significantly electron affinities of the EL polymers [3–6].

Polymers of fluorene derivatives (PFs) possess interesting and unique chemical and physical properties. They contain a rigid planar biphenyl unit, which provides efficient luminescence in the blue spectral region. The C9 position of fluorene is easily substituted and long alkyl substituted polymers have high solubility and processability. Their photo-stability and thermal stability are also found to be better than those of poly(phenylene vinylene)s (PPVs). As a result, polyfluorenes have been intensively studied recently as blue light-emitting materials[7,8]. Many fluorene copolymers have also been prepared to improve the efficiency by balancing the hole and electron injection and transport [9–13].

Phenoxazines usually have high luminescence quantum yields and are known as efficient laser dyes. The emission maximum of *N*-(4-*n*-butylphenyl)phenoxazine (PPX) is around 400 nm. Furthermore, the chemical structure of PPX resembles that of triphenylamine (TPA), which is widely used as a hole-transporting organic material. Thus, polymers containing a phenoxazine unit could be promising conducting and fluorescent materials.

In a paper about copolymers containing a phenoxazine derivative, PPX, and 9,9-dibutylfluorene (DBF) and fabricated an efficient EL device using this type of polymer[14]. In this

chapter, PPX and DBF copolymers with different ratio of monomers were prepared by oxidative polymerization using iron (III) chloride as an oxidant. The resulting copolymers were characterized with ^{1}H NMR, cyclic voltammetry (CV), and optical absorption and photoluminescence (PL) spectroscopy. The hole and electron mobilities were measured by time-of-flight method. A simple single layer EL device was fabricated, and the efficiency of the device is discussed in terms of the balance of hole and electron mobility.

4.2. Experimental

4.2.1. Materials

All chemicals were obtained commercially and used without further purification except otherwise noted. Xylene, tetrahydrofurane (THF), and toluene were dried by distilling over sodium. Tri-*tert*-butylphosphine was used as a 1 M xylene solution.

4.2.2. Synthesis of monomers

4.2.2.1. PPX

The synthesis route of *N*-4-butylphenlphenoxazine (PPX) is shown in Scheme 4-1a. A three-necked flask equipped with a magnetic stirrer and a Liebig condenser was loaded with phenoxazine (5 g, 0.0273 mmol), 1-bromo-4-*n*-butylbenzene (5.82 g, 0.0273 mmol), sodium *tert*-butoxide (3.15 g, 0.0328 mmol), and palladium(II) acetate (6.1 g, 0.0273 mmol). Xylene (40 mL) and a xylene solution of tri-tert-butylphosphine (0.11 mL, 0.1092 mmol) were added via a syringe, and the mixture was stirred under a nitrogen atmosphere for 3 h at 120^{o}C. After the reaction was terminated, the mixture was cooled, and water was poured into it. The organic layer was washed with water and concentrated by evaporation followed by purification with column chromatography. Recrystallization from acetone gave a white powder in a 91% yield. ^{1}H NMR [chloroform-d ($CDCl_3$), δ, ppm]: 0.95 (s, 3H), 1.40 (m, 2H), 1.70 (m, 2H), 2.75 (t, 2H), butyl protons; 5.90–7.40 (m, 12H), aromatic protons.^{13}C NMR ($CDCl_3$, δ, ppm): 13.9, 22.4, 33.5 (butyl), 113.3–144.1 (aromatics).

4.2.2.2. DBF

The synthesis route of 9,9-dibutylfluorene (DBF) is shown in Scheme 4-1b. A three-necked flask equipped with a magnetic stirrer and Liebig condenser was loaded with THF (320 mL) and fluorene (25 g, 0.150 mol), and the mixture was cooled while stirring to -78^{o}C. To the solution was added *n*-butyllithium (120 mL, 0.315 mol) dropwise over 1 h, followed by the addition of *n*-butylbromide (47.27 g, 0.345 mol). The mixture was warmed back to room temperature and stirred for 3 h. The organic layer was washed with water, dried with magnesium sulfate, concentrated by evaporation, and recrystallized from methanol. A white powder was obtained in a 54% yield.

^{1}H NMR ($CDCl_3$, δ, ppm): 0.60 (m, 4 H), 0.75 (s, 6H), 1.10 (m, 4H), 1.90 (m, 4H), butyl

protons; 7.2–7.8 (m, 8H), aromatic protons. ^{13}C NMR ($CDCl_3$, δ, ppm): 13.8, 23.1, 25.9, 40.2 (butyl); 54.9; 119.6–150.6 (aromatics).

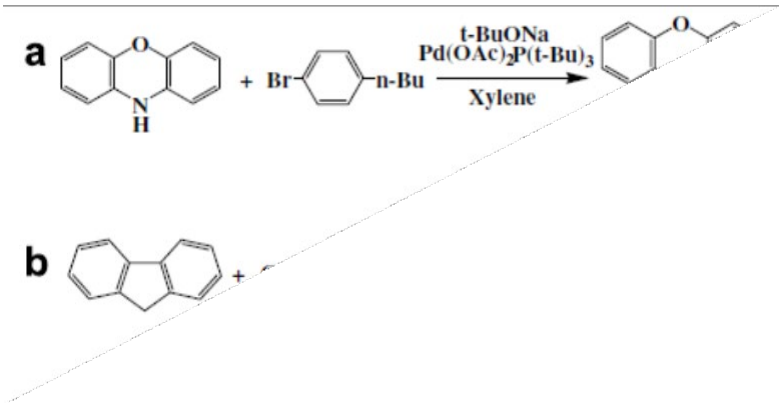

Scheme 4-1

4.2.2.3. Polymerization

Iron(III) chloride was dissolved in chloroform in a two-necked flask equipped with a magnetic stirrer and a Liebig condenser. PPX and DBF were added to the solution, and after the reaction time of 20 h a large amount of methanol was poured into it to terminate the reaction. The resulting brown precipitate was filtered, mixed with toluene, and separated by centrifugation into toluene-soluble and toluene-insoluble portions. The toluene-soluble portion was concentrated by evaporation and poured into large amount of methanol. The precipitate was then dissolved in toluene and reprecipitated into acetone. The precipitate was filtered and dried in vacuum, resulting in a brown powder.

4.2.3 Fabrication of the EL devices

Glass substrates with an indium tin oxide (ITO) electrode were cleaned by sonification in detergent,deionized water, isopropyl alcohol, and methanol and dried in a stream of nitrogen. The polymers were dissolved in toluene at concentrations of 30–50 mg/mL and spin-coated onto the substrates at 2000 rpm for 30 s. After drying, calcium (10 nm) as evaporated onto the polymer film at 1×10^{-4} Pa. Aluminum (100 nm) was coated on the cathode (Ca) by evaporation.

4.2.4. Instrumentation

NMR spectra were recorded on a JEOL α-500 spectrometer operating at 500 MHz (^1H), at 50°C, in $CDCl_3$ with tetramethylsilane as an internal standard. The molecular weights were determined by gel permeation chromatography (GPC) using a Jasco 880-PU pump, a column packed with styrene–

divinylbenzene gel beads, and a Jasco UV-970 detector. Chloroform was used as an eluent, and the molecular weight was calibrated with polystyrene standards. The glass transition temperatures were measured with a Rigaku Thermo DSC 8230 differential scanning calorimeter at a scanning rate of 10 K/min. CV measurements were carried out in a nitrogen atmosphere in a one-compartment cell with a Toho PS-06 polarization unit with polymer films cast onto a carbon electrode. Dry acetonitrile containing 0.1 M tetra-*n*-butylammonium bromide was used as an electrolyte, a platinum spiral was used as a counter electrode, and Ag/AgCl was used as a reference electrode. The scanning rate was 20 mV/s. Ultraviolet–visible (UV–vis) absorption spectra were measured on a Jasco Ubest-30 spectrometer, and PL and EL spectra were measured on a Jasco FT-6500 spectrofluorometer. The charge mobility was determined via time-of-flight photocurrent experiments using a device consisting of ITO glass/polymer/Al. The EL devices were characterized with a Kenwood PSR-60M power supply, an Advantest R5451 multimeter, and a Minolta LS-100 luminance meter.

4.3. Results and discussion

4.3.1. Polymer synthesis

PPX and DBF copolymers were synthesized via an oxidative coupling reaction with iron(III) chloride. The reaction conditions and the synthesis results are summarized in Table 3-1. The toluene soluble portion increased and insoluble portion decreased with the increase of PPX fraction in feed. The total yield stayed in the range of 74–83% with the PPX percentage in feed up to 50%. When PPX content was higher than 70%, no polymer was obtained. It is found that only chlorinated PPX at 3 and 7 potions was obtained by the reaction of PPX with $FeCl_3$. Therefore, it is estimated that only chlorinated low molecular weight compounds were obtained at high PPX feed. The molecular weight changed only slightly with the change of PPX content in feed.

The structure of the polymers was determined by ^{1}H NMR. Fig. 4-1 shows typical ^{1}H NMR spectra of the polymer obtained. The signals in the range of 0.7–2.7 ppm were attributed to butyl chain protons of both PPX and DBF units; the multiplet signals between 5.8 and 8.8 ppm were assigned to

Table 4-1. Polymerization conditions and results[a]

PPX in feed (%)	Yield (%)		$M_n/10^4$	$M_w/10^4$	PDI	PPX inpolymer (%)[c]
	Soluble[b]	Insoluble[b]				
0	24.3	58.3	1.1	2.4	2.2	0
10	49.7	31.3	1.1	2.3	2.1	8
20	56.3	18.1	1.0	2.1	2.1	17
34	63.6	10.7	1.1	2.6	2.4	30
50	72.9	6.9	1.0	2.3	2.3	42
65	1.0	0.0	0.1	0.2	2.0	–
70	0.0	0.0	–	–	–	–

[a] Polymerization was carried out in chloroform with total monomer concentration of 0.20 M with the molar ratio of monomer to iron(III) chloride of 4.0 at 50 °C for 20 h.
[b] Yield of toluene soluble and insoluble portion.
[c] PPX fraction in polymer determined by ^{1}H NMR.

the aromatic protons of both units. The butyl proton signals were used to determine the fraction of PPX unit in the copolymers. The PPX content in the polymer, the last column of Table 4-1, was about 80–90% of PPX monomer in feed, which indicates that PPX had slightly lower reactivity than DBF monomer.

Fig. 4-1. ^{1}H NMR spectra of PPX and DBF copolymers along with the signal assignment.

4.3.2. Properties of polymers

Glass transition temperature (T_g) limits the operation temperature of the device prepared. Glass transition temperature (T_g) of the synthesized polymers was determined by DSC. The observed values are listed in the second column of Table 4-2. All polymers had T_g in the range from 157 to 176°C, indicating morphological stability at high temperature.

Figure 4-2 shows UV–vis absorption spectra of the polymers in THF. PolyDBF showed absorption maximum at 367 nm. The absorption maximum shifted to the longer wavelengths with the increase of PPX content. The polymer containing 42% of PPX units showed absorption maximum at 402 nm. Similar red-shift was observed for photoluminescence (PL) spectra, as shown in Fig. 4-3. Poly- DBF exhibited a PL peak at 417 nm. The peak at 417 nm decreased rapidly with the increase of PPX unit content. A new PL peak corresponding to PPX unit appeared at 444 nm in the spectrum of the polymer containing 8% of PPX unit. This peak shifted to the longer wavelength with the increase of PPX unit. The polymer containing 42% of PPX unit showed the peak at 458 nm.

Table 4-2. Physical properties of polymers

PPX unit in polymer (%)	T_g[a] (°C)	Epa[b] (eV)	Epc[b] (eV)	HOMO[c] (eV)	LUMO[d] (eV)	Eg[e] (eV)
0	176.2	−1.61	1.64	−6.33	−3.10	−3.23
8	163.4	−1.40	1.45	−6.12	−2.96	−3.16
17	157.5	−1.27	1.29	−5.99	−2.92	−3.07
30	161.7	−1.11	1.07	−5.83	−2.85	−2.98
42	160.6	−1.07	1.05	−5.79	−2.83	−2.96

[a] Glass transition temperature determined by DSC.
[b] Oxidation (Epa) and reduction (Epc) potentials determined by cyclic voltammetry.
[c] Highest occupied molecular orbital level calculated from Epa.
[d] Lowest unoccupied molecular orbital level calculated by adding Eg to HOMO.
[e] Band gap energy determined from cut-off wavelength of UV absorption spectra.

Chloroform solutions of the polymers were cast on a platinum electrode and the cyclic voltammograms were measured in acetonitrile containing 0.1 M tetrabutylammonium perchlorate as an electrolyte. The oxidation and reduction potentials are listed in Table 4-2. Oxidation potential decreased with the increase of PPX unit content, as expected. It is noteworthy that all the polymers had reduction peaks as well as oxidation ones, indicating that the polymers may have electron and hole mobility. Energy level of the highest occupied molecular orbital (HOMO) was estimated from the oxidation potential by adding energy level of normal hydrogen electrode (-4.50 eV) and that of reference electrode of Ag/AgCl (-0.22 eV). Energy level of the lowest unoccupied molecular orbital (LUMO) was calculated from HOMO level and band gap energy obtained from cut-off wavelength of UV spectra. These energy levels are tabulated in Table 4-2. HOMO and LUMO levels increased with the increase of PPX content.

Fig. 4-2. UV absorption spectra of polymers.

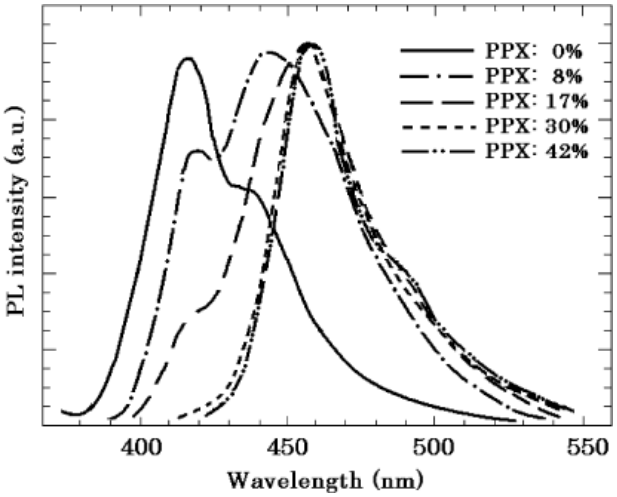

Fig. 4-3. PL spectra of polymers

The hole and electron drift mobility were measured by the standard time-of-flight method using a device consisting of ITO glass/polymer/Al. The hole (μ_h) and electron mobilities (μ_e) were calculated according to the following equation:

$$\mu = L^2 / t_T V$$

where L is the sample thickness, t_T is the transit time, and V is the applied voltage. The t_T is determined from the transit time determined using double-logarithmic plots of current i versus time t. The values

of hole and electron mobility are shown in Table 4-3. Hole mobility increased and electron mobility decreased with the increase of PPX unit content. These results clearly indicate that hole was mainly transported by the PPX unit, while electron mainly by the DBF unit.

Table 4-3 Hole and electron mobility of polymer films

PPX content (%)	Film thickness (μm)	Hole mobility μ_h ($cm^2/V\,s$)	Electron mobility μ_e ($cm^2/V\,s$)	μ_e/μ_h
0	1.9	2.6×10^{-6}	7.3×10^{-5}	28.1
8	1.6	8.2×10^{-6}	5.8×10^{-5}	7.07
17	1.8	9.7×10^{-6}	4.3×10^{-5}	4.43
30	1.7	2.4×10^{-5}	2.6×10^{-5}	1.08
42	1.9	3.7×10^{-5}	1.6×10^{-5}	0.43

Fig. 4-4. Current–voltage (left) and luminance–voltage(right) characteristics of EL device with the structure of ITO/polymer/Ca/Al.

4.3.3. Properties of EL device

A single-layer EL device was prepared using ITO as a cathode and calcium–silver (10-1) as an anode and using polymer film with thickness of about 100 nm. Calcium was used as an anode because it has low work function, which facilitates electron injection. Figs. 4-4a and b show current density–voltage

Table 4-4 Properties of EL device consisting of ITO/polymer/Ca/Al

PPX content (%)	V turn-on (V)	Max brightness (cd/m2)	Current density[a] (mA/cm^2)	Current efficiency[b] (cd/A)
0	5.5	61	280	0.02
8	6.0	208	369	0.05
17	4.5	281	321	0.08
30	4.5	1084	342	0.32
42	5.0	581	350	0.16

[a] current density at the maximum brightness.
[b] current efficiency at the maximum brightness.

and luminance–voltage curve characteristics, respectively. Properties of the EL device are tabulated in Table 4-4. Polymer containing only DBF showed the lowest brightness of all devices with the value of 61 cd/m^2 at the current density of 280 mA/cm^2. The brightness increased with PPX unit content up to 30% and decreased after that. The polymer containing 30% of PPX unit showed maximum brightness of 1084 cd/m^2 and current efficiency of 0.32 cd/A at the current density of 342 mA/cm^2. These results indicate that at the low PPX unit content electron transporting was faster than hole-transporting leading to an excess of electrons that reached the anode without recombining with a hole. With higher PPX content, an excess of holes was transported. In the polymer containing 30% of PPX unit, electrons and holes were balanced, leading to the highest current efficiency. The efficiency is also affected by the cell structure. If more complex structure, for example, double- or triple-layer structure by introducing hole or electron injection layer is used, higher efficiency may be expected. The maximum brightness of 1084 cd/m^2 and current efficiency of 0.32 cd/A are one of the highest for single-layer device.

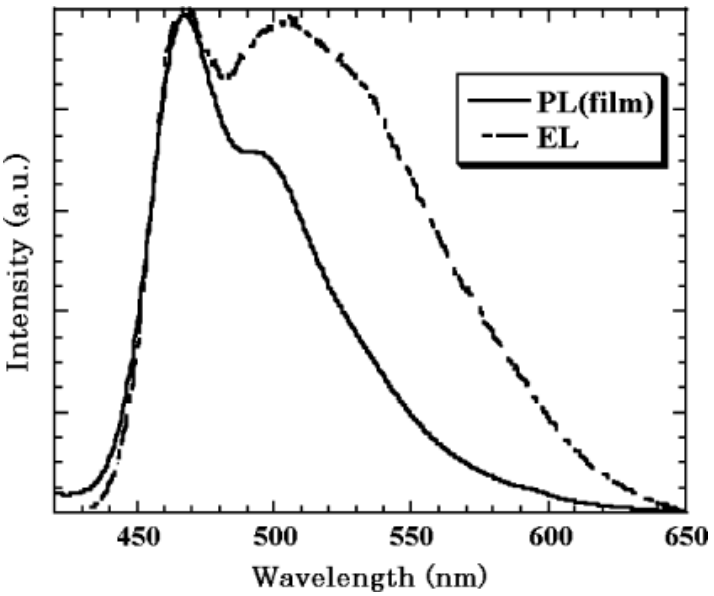

Fig. 4-5. PL and EL spectra of the polymer (PPX 30%).

Figure 4-5 shows PL spectrum of a polymer film and EL spectrum of an EL device. In comparison with the solution spectra of Fig. 4-3, the film PL spectrum exhibited a new peak around 500 nm. This peak increased greatly in the EL spectrum. This peak can be attributed to eximer emission. Similar new emission was observed for an EL device prepared with PF containing oxadiazole or triphenyl amine units[13].

4.4. Conclusion

Polymers containing fluorene and phenoxazine units were prepared by oxidative polymerization of DBP and PPX. With the increase of PPX unit oxidation potential of the polymer decreased. Hole mobility increased from 2.6×10^{-6} to 3.7×10^{-5} cm^2/Vs and electron mobility decreased from 7.3×10^{-5} to 1.6×10^{-5} cm^2/Vs as PPX content increased from 0% to 42%. EL device

with the structure of ITO/Polymer/Ca/Al was fabricated. With polymer containing 30% of PPX units, the device showed best properties: maximum luminance of 1084 cd/m^2 and current efficiency of 0.30 cd/A.

References

1) J.H. Burroughes, D.D.C. Bradley, A.R. Brown, R.N. Marks, K. Mackay, R.H. Friend, P.L. Burn, A.B. Holmes, *Nature* **347** (1990) 539–541.

2) N.C. Greenham, S.C. Moratti, D.D.C. Bradley, R.H. Friend, A.B. Holmes, *Nature* **365** (1993) 628–630.

3) Z. Wang, X. Yang, X. Chen, Z. Xu, X. Xu, *Thin Solid Films* **63** (2000) 94–97.

4) S.-H. Jin, M.-Y. Kim, J.Y. Kim, K. Lee, Y.-S. Gal, *J. Am. Chem. Soc*. **126** (2004) 2474–2480.

5) D.W. Lee, K.-Y. Kwon, J.-I. Jin, Y. Park, Y.-R. Kim, I.-W. Hwang, *Chem. Mater.* **13** (2001) 5650574.

6) S.-J. Lee, J.R. Gallegos, J. Klein, M.D. Curtis, J. Kanicki, *Synth. Met.* **155** (2005) 1–10.

7) M. Leclerc, *J. Polym. Sci. Part A: Polym. Chem.* **39** (2001) 2867–2873.

8) U. Scherf, E. List, *Adv. Mater* **14** (2002) 477–487.

9) L.J. Lindgren, F. Zhang, S. Admassie, X. Wang, M.R. Andersson, O. Inganaes, *J. Lumin.* **122–123** (2007) 610–613.

10) E. Lim, B.-J. Jung, H.-K. Shim, *J. Polym. Sci., Part A:Polym. Chem.* **44** (2006) 243–253.

11) D.-H. Hwang, S.-K. Kim, M.-J. Park, J.-H. Lee, B.-W. Koo, I.-N. Kang, S.-H. Kim, T. Zyung, *Chem. Mater.* **16** (2004) 1298–1303.

12) A.J. Campbell, D.D.C. Bradley, T. Virgili, D.G. Lidzey, H. Antoniadis, *Appl. Phys. Lett.* **79** (2001) 3872–3874.

13) Q. Sun, X. Zhan, C. Yang, Y. Liu, Y. Li, D. Zhu, *Thin Solid Films* **440** (2003) 247–254.

14) Y. Ito, T. Shimada, J. Ha, M. Vacha, H. Sato, *J. Polym.Sci., Part A, Polym. Chem.* **44** (2006) 4338.

Chapter 5 Synthesis of Polymer having Thioxanthene Unit in Main Chain and Application to Photorefractive Composites

ABSTRACT

Poly (arylene ether) was successfully synthesized from 2,7-dichloro-9*H*-thioxanthen-9-one- 10,10-dioxide and bisphenol-A by a nucleophilic substitution reaction. The resulting polymer had a weight average molecular weight of 11,000 and exhibited a glass transition temperature of 184 °C. Photorefractive composites consisting of the synthesized polymer as an electron transporting component and electro-optically active 4-*N,N*-diethylamino- -nitrostyrene (DEANST) were prepared. A PR device with a thickness of 100 m was fabricated by sandwiching the PR composite between two indium-tin-oxide covered glasses. The electric field dependences of the gain coefficient and diffraction efficiency were investigated by two-beam coupling and four-wave mixing experiments, respectively. Compared with the composite with polyacrylate containing more electro accepting thioxanthene unit, the composite base on the synthesized polymer exhibited a higher diffraction efficiency and a larger net gain because of a weaker absorption although a slower response was observed.

5.1. Introduction

Electron transporting polymers have been synthesized[1-3], and first reported the PR composites consisting of an electron transporting host polymer, which is acrylate polymer containing thioxanthene derivative on the side chain (P-THEA), and EO active 4-*N,N*-diethylamino-β-nitrostyrene (DEANST)[4]. It was found that durability of PR devices greatly extended due to the better compatibility of P-THEA and DEANST. Enhanced compatibility was mainly attributed to the electrical interaction between electron accepting P-THEA and electron donating DEANST. This interaction also resulted in the absorption at 633 nm (He-Ne laser) although both P-THEA and DEANST are inherently transparent at that wavelength. The charge transfer interaction made photocharge generation possible without a photosensitizer. Although 64 cm^{-1} of two-beam coupling gain at 50 V/ μm was obtained for P-THEA/DEANST (70/30), the net gain was only 31 cm^{-1} because of the large absorption. Therefore, it is important to utilize a host polymer that interacts electrically with EO chromophore to a lesser extent in order to fabricate an efficient PR device.

In chapter, poly (arylene ether) containing electron transporting thioxanthene unit in main chain was prepared and characterized. It was applied to the host polymer of PR composite. In this polymer electron donating ether oxygen atoms attach to thioxanthene moiety. Therefore, it is expected that the absorption coefficient decreases since the overall electron accepting nature of thioxanthene moiety can be suppressed. PR characteristics were investigated by two-beam coupling and four-wave mixing experiments.

5.2. Experimental

5.2.1 Monomer Synthesis

Synthesis of monomer having thioxanthene was conducted as shown in Scheme 5.1. All reagents were obtained commercially and used as received otherwise noted.

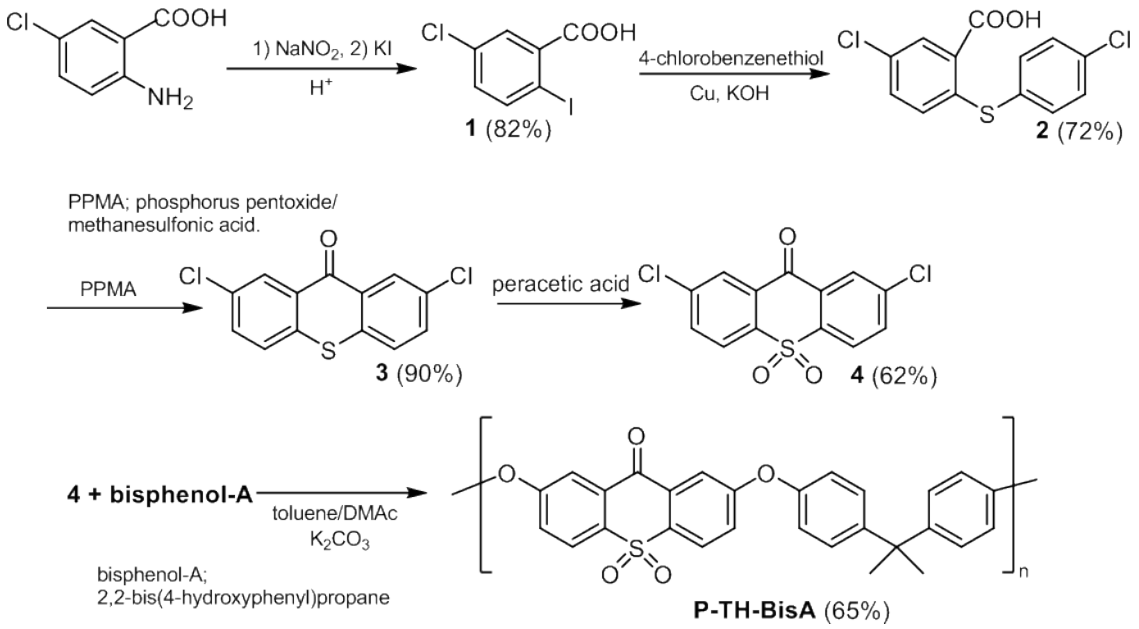

Scheme 5.1 Synthetic route of P-TH-BisA

5-chloro-2-iodobenzoic acid (1)

Into a 200-mL three-necked flask fitted with a mechanical stirrer, a condenser, and a thermometer, 15.2 g of concentrated hydrogen chloride, 40 mL of distilled water and 5.0 g (0.029 mol) of 2-amino-5-chlorobenzoic acid was added. Reaction vessel was cooled with an ice bath, and a chilled solution of 2.1 g of sodium nitrite in 10 mL of distilled water was dropwise added fast enough not to cause the temperature to rise to 5 °C. After stirring was continued for 30 min, an aqueous solution of 4.85 g (0.029 mol) of potassium iodide in 8.0 mL of water was added, and the reaction mixture allowed to stand overnight at room temperature followed by raising the temperature to 90 °C for 6 h until no more gas was evolved. After cooling, the precipitate was collected by filtration, and was washed with water. Crude product was recrystallized in water/ethanol to yield 6.7 g (82%) of the product. ^{1}H NMR (300 MHz, DMSO-d_6) δ 7.97 (d, J=8.2 Hz, 1H), 7.70 (d, J=2.4 Hz, 1H), 7.30 (dd, J_1=8.2 Hz, J_2=2.4 Hz, 1H); ^{13}C-NMR (75 MHz, DMSO-d_6) δ 166.2, 141.6, 138.5, 132.8, 131.5, 129.0, 90.9.

4-chloro-2-[(5-chlorophenyl)thio]benzoic acid (2)

Into a 1000-mL three-necked flask fitted with a mechanical stirrer and a condenser, 56.6 g (39.1 mmol) of 4-chlorobenzenethiol, 110 g of **1**, 74.1 g of potassium hydroxide, 2.73 g of cupper

powder and 780 mL of distilled water were added. The reaction mixture was refluxed for 12 h. After cooling, the solution was filtered to remove cupper powder, and the filtrate was acidified with concentrated hydrogen chloride to precipitate the product. After filtration and washing with water, the crude product was recrystallized in acetic acid to yield 83.3 g (72 %) of the product. ^{1}H NMR (300 MHz, $CDCl_3$) δ 11.0 (br. 1H, COOH), 8.06 (d, *J*=2.4 Hz, 1H), 7.46 (d, *J*=6.4 Hz, 2H), 7.40 (d, *J*=6.4 Hz, 2H), 7.25 (dd, J_1=8.9 Hz, J_2=2.4 Hz, 1H), 6.76 (d, *J*=8.9 Hz, 1H). ^{13}C-NMR (75 MHz, $CDCl_3$) δ 170.2, 142.3, 136.7, 136.0, 133.2, 131.8, 130.8, 130.2, 129.5, 128.9, 127.1.

2,7-dichloro-9*H*-thioxanthen-9-one (3)

Into a 50-mL three-necked flask fitted with a magnetic stirrer, a condenser, and nitrogen inlet, 1.02 g (3.41 mmol) of **2** and 1 g of phosphorous pentaoxide dissolved in 9 mL of methane sulfonic acid were added. After stirring for 4 h at 80 °C, the reaction mixture was poured into 200 mL of distilled water. The precipitate was washed with saturated sodium carbonate solution and water, successively. After drying, the product was recrystallized in ethanol to yield 0.86 g (3.06 mmol, 90 %) of yellow crystalline. ^{1}H NMR (300MHz, $CDCl_3$) δ 8.57 (d, *J*= 2.1 Hz, 2H), 7.59 (dd, J_1= 8.5 Hz, J_2=2.1 Hz, 2H), 7.52 (d, *J*= 8.5 Hz, 2H); ^{13}C-NMR (75 MHz, $CDCl_3$) δ 177.9, 135.2, 133.2, 132.9, 130.1, 129.6, 127.5.

2,7-dichloro-9*H*-thioxanthen-9-one-10,10-dioxide (4)

Into a 100-mL three-necked flask fitted with a magnetic stirrer, a condenser, and nitrogen inlet, 0.5 g (1.78 mmol) of **3** and 6 mL of peracetic acid solution (32 wt % in aqueous acetic acid) were added. After stirring for 3 h at 70 °C, the precipitate was collected and washed with water. The crude product was recrystallized in toluene to yield 0.37 g of slightly yellow colored needle crystal (66%). ^{1}H NMR (300MHz, $CDCl_3$) δ 8.29 (d, *J*=2.2 Hz, 2H), 8.11 (d, *J*= 8.6 Hz, 2H), 7.84 (dd, J_1=8.6 Hz, J_2=2.1 Hz, 2H); ^{13}C NMR (75 MHz, $CDCl_3$) δ 176.5, 140.5, 139.3, 134.9, 131.8, 129.3, 125.4. HRMS (APCI) m/z: [M+H]+ Calculated for $C_{13}H_7Cl_2O_3S$ 312.9485; Found 312.9487.

5.2.2 Polymerization

Nucleophilic substitution polymerization was carried out according to the literature as shown in Scheme 1[5]. Into a 100-mL three-necked flask fitted with a magnetic stirrer, a nitrogen inlet, Dean-Stark trap, 1.000 g (3.193 mmol) of **4** and 0.729 g (3.193 mmol) of 2,2-bis(4-hydroxyphenyl)propane (bisphenol-A), 0.660 g (4.775 mmol) of potassium carbonate, 7.0 mL of *N*, *N*-dimethylacetamide (DMAc) and 7.0 mL of toluene were charged. The reaction mixture was heated at 120 °C for 10 h, and then was poured into 140 mL of water-methanol mixture (1:1) to precipitate the polymer. The recovered polymer was washed with aqueous methanol and water successively, and then was purified by reprecipitation of a chloroform solution into methanol, followed by drying in vacuo. Slightly brownish powder (0.97 g) was obtained in a yield of 62%.

5.2.3 Measurements.

NMR spectra were recorded at 50 °C (for $CDCl_3$ solution) or 70 °C (for DMSO-d_6 solution)

with a JNM-ECX300 spectrometer (JEOL Ltd., Japan) operating at 300 MHz for ^{1}H, and at 75 MHz for ^{13}C. UV spectra were obtained for chloroform solutions or cast films with a JASCO V-500 UV / VIS / NIR spectrometer. Mass spectra was record on a micrOTOF-Q II (Bruker Co., the U.S.) with a direct inlet probe-atmospheric pressure chemical ionization method. The molecular weights of synthesized polymers were estimated by gel permeation chromatography using a column packed with styrene-divinylbenzene gel beads[6]. Chloroform was used as an eluent and the molecular weight was calibrated using polystyrene standards (Shodex). Glass transition temperature (T_g) was determined from differential scanning calorimetry (DSC) chart that was recorded by SEIKO Instruments DSC 220 under nitrogen at heating rate of 10 °C /min. Redox potentials were measured with cyclic voltammetry in a one-compartment cell with a polarization unit (TOHO PS-06). The measurements were conducted for the cast films on platinum working electrode in dry acetonitrile containing tetrabutylammonium perchlorate (0.1 M) as an electrolyte under nitrogen atmosphere. Platinum spiral was used as a counter electrode, and Ag /AgCl as a reference electrode.

5.2.4 PR sample preparation and measurements

PR devices were fabricated as follows. The mixture of the prepared polymer (P- TH-BisA) and 4-*N,N*-diethylamino-*β*-nitrostyrene (DEANST) which was prepared according to the literature[7], was dissolved in 1,2-dichloroethane. Some composites contained 9-oxo-9*H*-thioxanthene-3-butoxycarbonyl-10,10-dioxide (TH-Bu) as the additional component. All the chemical structures of materials used for PR composites are shown in Fig. 5.1. The solution was filtered through 0.5 μm filter and then heated to 40 °C for solvent evaporation until highly viscous solution was obtained. The resulting solution was dripped on indium tin oxide (ITO, 30Ω/□) covered glass substrate. After the evaporation of solvent, sample was heated with hot plate at about 70 °C at which the composite was soften. The composite was sandwiched with another ITO covered glass. The sample thickness was controlled to be approximately 100 μm with the use of Teflon spacer.

Photorefractive properties were studied by the two-beam coupling (2BC) and four wave mixing (FWM) techniques. Holographic grating was written using coherent beams from an NEC GLS-5410 He-Ne laser operating at 633 nm. All experiment were carried out at room temperature(22 ± 2°C). The detailed experimental geometry for the 2BC and FWM experiment is described . In 2BC experiments, the incoming laser beam (*p*-polarized) was split into two writing beams (beam 1 and beam 2) with equal intensity (130 mW/cm^2). The two writing beams with an angle of 20° were directed onto the sample which was tilted at an angle of 50° with respect to the bisector of the two writing beams to achieve a nonzero projection of the EO coefficients. The transmitted beam intensities were monitored with photodiodes (Hamamatsu Photonics, S2281). In the FWM experiments, two *s*-polarized beams of equal intensity (130 mW/cm^2) wrote a grating, which was probed by a much weaker *p*-polarized beam (0.8 mW/cm^2) counter-propagating to one of the writing beams.

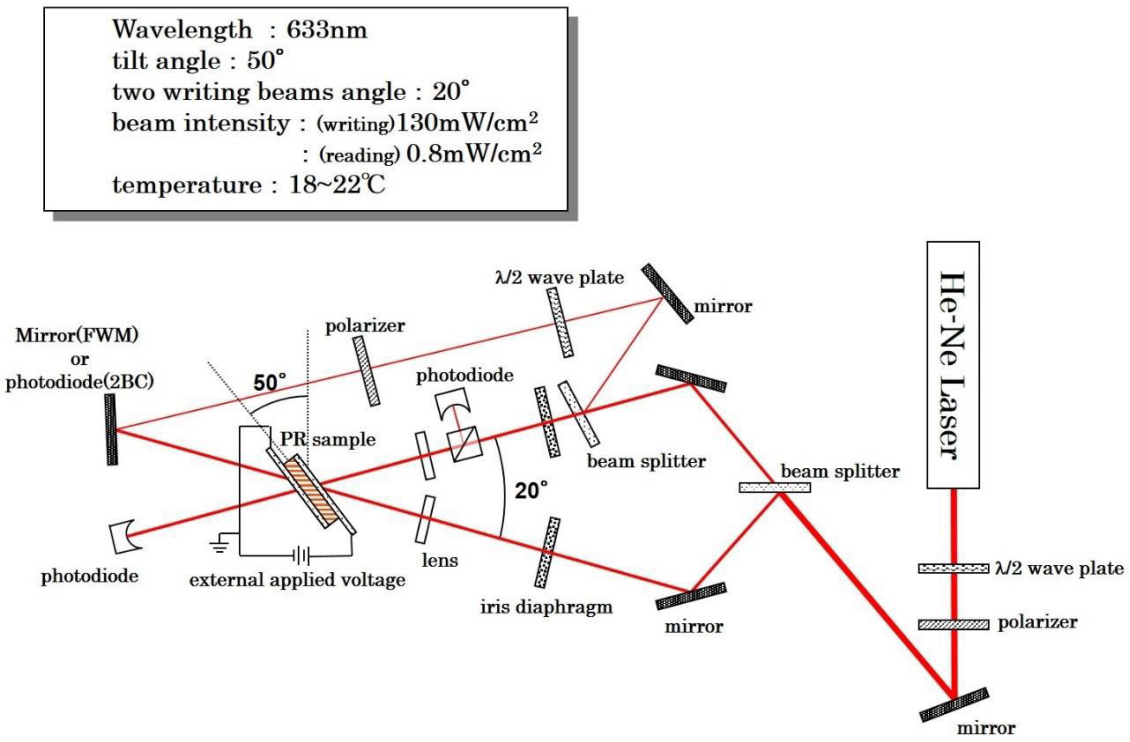

Fig. 5.1 Schematic representation of setup for PR measurements

5.3 RESULTS AND DISCUSSION

5.3.1 Characterization of Polymer and PR Composite

Synthesized dichloride (**4**) was successfully polymerized with bisphenol-A via a nucleophilic substitution reaction. The monomer has electron withdrawing carbonyl group and sulfonyl group at *p*-position to chloride, which facilitated the elimination of chlorides. Fig. 5.2 shows the ^{1}H-NMR spectrum of the prepared polymer (P-TH-BisA), where all the signals were assigned to the protons in the expected structure. P-TH-BisA had the number- and weight-average molecular weights of 5,100 and 10,700, respectively, and was soluble in a variety of organic solvents such as chloroform, 1,2-dichloroethane, tetrahydrofuran, dimethylformamide, and DMAc. The glass transition temperature (T_g) was 184 °C. P-TH-BisA had UV absorption maximum at 334 nm in 1,2-dichloroethane. Compared with a polyacrylate with a thioxanthene moiety as a pendant group (P-THEA [4]) in Fig. 5.3), ca. 50 nm of red-shift was observed, which can be attributed to the intramolecular charge-transfer between electron-donating ether oxygen and electron-withdrawing sulfone group, which are located *p*-position each other in the thioxanthene moiety.

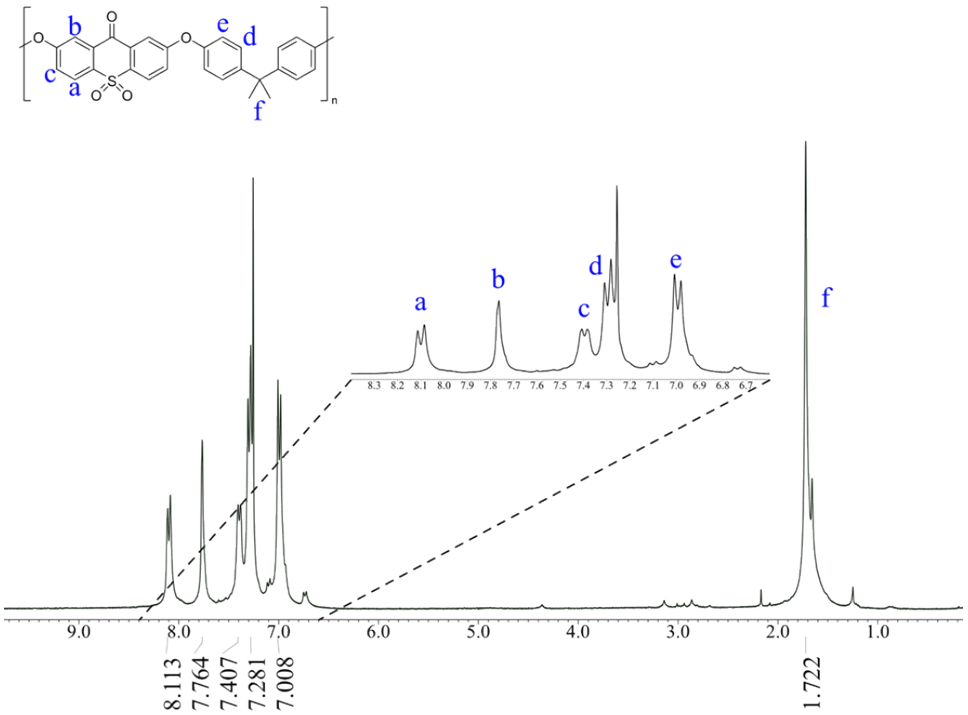

Fig. 5.2 ^{1}H-NMR spectrum of P-TH-BisA in $CDCl_3$ at 300 MHz.

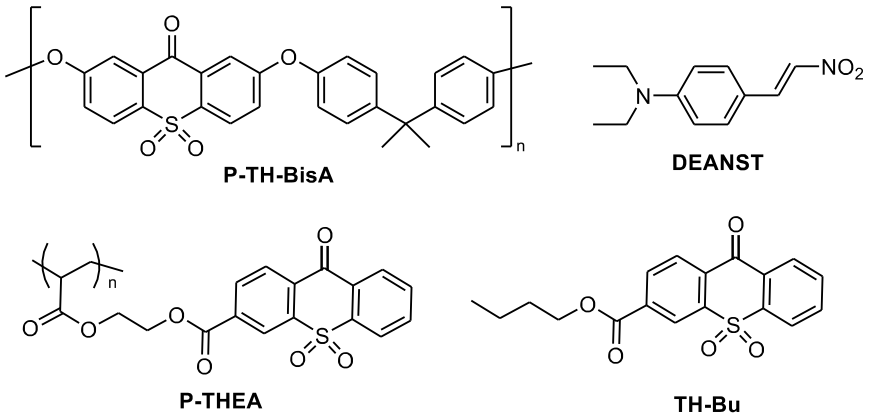

Fig. 5.3 Chemical structure of compounds used in this study.

Table 5.1 shows the absorption coefficients at 633 nm and T_g of composites based on P-TH-BisA with 100 μm thickness. For the comparison, the data for the composites based on P-THEA were also tabulated. The absorption coefficient of the composite increased with DEANST concentration. The composite consisting of poly(methyl methacrylate) and DEANST showed the absorption coefficients of 1.0 and 1.3 cm^{-1} for those containing 20 and 30 wt% of DEANST, respectively. Larger absorption was observed in P-TH-BisA/DEAST composite, which is attributed to the intermolecular charge transfer interaction between both components, *i.e.*, electron donating DEANST and electron accepting thioxanthene moiety in the polymer[4]. The charge transfer complex can play a role of

photocharge generator, therefore our composite would have the ability of charge generation without adding any charge generator or photosensitizer. It is also expected that the specific interaction increases the solubility of the dopant, and the morphologycal stability of a composite[4]. Higher was the content of compounds with low molecular mass, the lower was T_g of the composite. Compared with P-THEA based composites, the higher T_gs were observed in composites based on P-TH-BisA due to the higher T_g of original polymer (184 °C).

Table 5.1 Characteristics of homopolymers and composites

material	wt%	T_g (°C)[a]	α (cm^{-1})[b]	Γ (cm^{-1})[c]	η (%)[d]	τ (s)[e]
P-TH-BisA	100	184	0	n.d.	n.d.	n.d.
P-TH-BisA/DEANST	70/30	55	7	71	11.1	7.0
P-TH-BisA/DEANST	80/20	71	4	n.d.	1.4	5.5
P-TH-BisA/DEANST	60/30/	43	13	n.d.	n.d.	n.d.
/TH-Bu	10					
P-THEA[f]	100	113	0	n.d.	n.d.	n.d.
P-THEA/DEANST[f]	70/30	42	33	64	5.4	0.2

a; glass transition temperature, b; absorption coefficient at 633 nm, c; gain coefficient at 50 V/μm, d; diffraction efficiency at 50 V/μm, e; response time at 50 V/μm, f; ref. 4.

It is noteworthy that absorption was suppressed compared with P-THEA based composite. In P-TH-BisA, electron donating ether oxygen atoms attached to thioxanthene moiety exist. Therefore, it is assumed that the overall electron accepting nature of thioxanthene moiety decreased compared with P-THEA, in which electron-withdrawing carbonyl group is attached to thioxanthene moiety. As shown in Table 5.1, the replacement of P-TH-BisA by TH-Bu, of which electro-optical data are similar to P-THEA, enlarged absorption. Electron-accepting nature was evaluated using cyclicvoltammetry. In Fig. 5.4 the cyclicvoltammograms of both the P-TH-BisA and P-THEA are depicted. For both polymers well-defined reversible redox waves. The reduction potential of P-TH-BisA was slightly lower indicating weaker electron accepting nature compared with P-THEA as predicted from chemical structures. It is possible that low absorption would afford an efficient PR device showing large net gain, and high external diffraction efficiency.

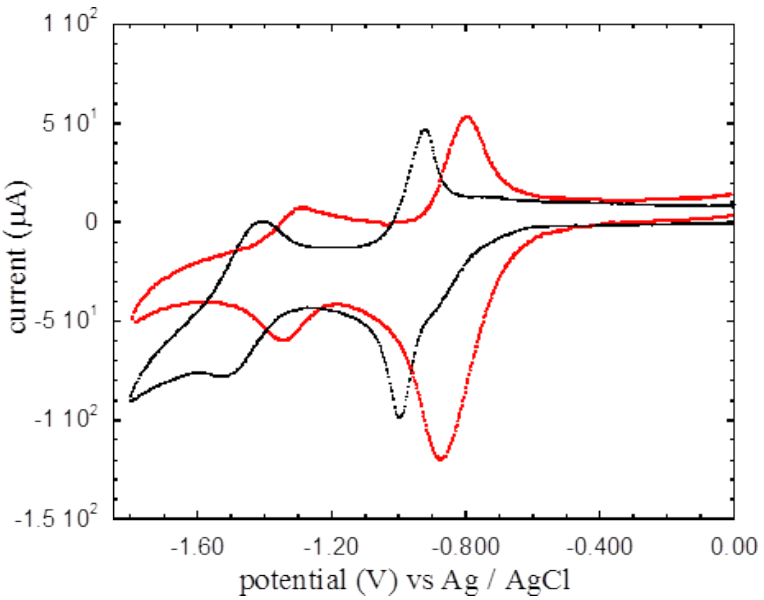

Fig. 5.4 Cyclic voltammograms of P-TH-BisA (black) and P-THEA (red).

5.3.2 Two beam coupling (2BC)

In order to verify the photorefractivity of the composites, 2BC experiments was performed. Asymmetric energy transfer was observed for devices based on both compounds. The 2BC-gain coefficient Γ was calculated from the following equation,

$$\Gamma = (L)\ \ln[\gamma\beta/(\beta + 1 - \gamma)]$$

where L is the optical path, β is the intensity ratio of the two incident beams, and $\gamma = I/I_0$ is beam coupling ratio where I_0 is the detected signal intensity without the pumping beam, and I is the intensity with pump beam.

Figure 5.5 shows the dependency of the applied voltage on the coupling gain observed in P-TH-BisA and P-THEA based composites with the polymer/DEANST was 70/30 by weight. As observed in general organic PR materials, Γ values increased quadratically with the applied voltage (or electric field). Both composites exhibited the similar profiles suggesting that Γ values are determined by the content of EO chromophore despite the higher T_g of P-TH-BisA/DEANST composite. Because of the difference of absorption coefficients, the net gain ($\Gamma - \alpha$) in P-TH-BisA/DEANST composite at 50 V/μm (5 kV) was 64 cm^{-1}, higher that that of P-THEA/DEANST (31 cm^{-1}) [4].

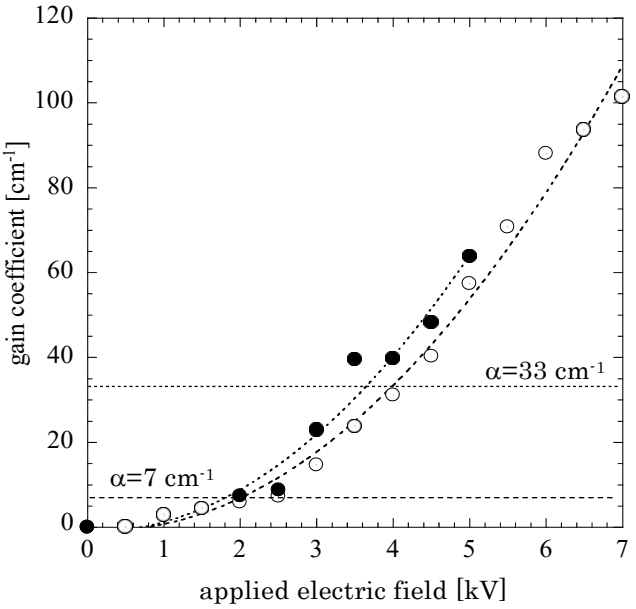

Fig. 5.5 Dependencies of applied electric field on gain coefficients.
Filled and open circles represent gain coefficients for devices based on P-TH-BisA / DEANST (70 / 30) and P-THEA /DEANST (70 / 30), respectively. Horizontal dotted lines show absorption coefficients of devices (α cm^{-1})

3.3 Four Wave Mixing

Figure 5.6 shows the electric field dependencies of the steady-state diffraction efficiency. Diffraction efficiency (h%) was determined by the following equation.

$$\eta(\%) = I_d/I_p \times 100$$

where I_d and I_p are beam intensities of diffracted and probe beams, respectively. The diffraction efficiencies increased with the applied electric field and reached maximum values more apparently in P-TH-BisA/DEANST. The higher diffraction efficiency was observed in P-TH-BisA/DEANST. As is obvious from the above equation, diffraction efficiency is determined based on the intensity of the probe beam (I_p). The intensity of diffracted beam (I_d) decreases by the absorption. As mentioned above, P-THEA/DEANST exhibited the stronger absorption. That is why the higher diffraction efficiency was observed in P-TH-BisA/DEANST even though the similar coupling gain was observed under the examined electric field.

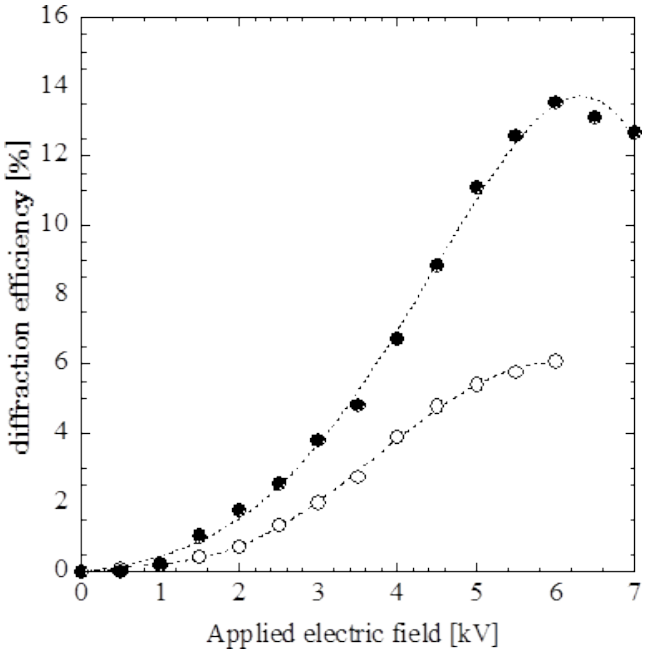

Fig. 5.6 Dependencies of applied electric field on diffraction efficiencies.
Filled and open circles represent diffraction efficiencies for devices based on P-TH-BisA / DEANST (70 / 30) and P-THEA /DEANST (70 / 30), respectively.

5.3.4 Response rate

The response time of PR grating formation was measured as follows. One writing beam and the reading beam illuminated the sample and the field was applied. After 60 s, the second writing beam illuminated the sample, and the buildup of the diffracted reading beam was monitored. By a curve fitting using the following, a response rate ($1/\tau$) is evaluated by the following equation[4],

$$\eta(t) = \eta_0 \left[1 - \exp\left(-\frac{t}{\tau}\right)\right]$$

where $\eta(t)$ and η_0 are diffraction efficiencies at time t, and steady state, respectively, and τ is a response time. The response rate increased as the electric field increased in all the devices examined as shown in Fig. 5.7 Devices based on P-TH-BisA/DEANST exhibited slower response compared with that of P-THEA/DEANST when the content of DEANST was 30 wt% due to the low absorption resulting in the low efficiency of photocarrier generation. As shown in Fig.5.7 and Table 5.1, with the 20 wt% of DEANST, the device showed similar response behavior to that of 30 wt%. This result also suggests the photocarrier generation process is rate-determining. Carrier drift and/or diffusion is generally improved with the decrease of DEANST content resulting in faster response.

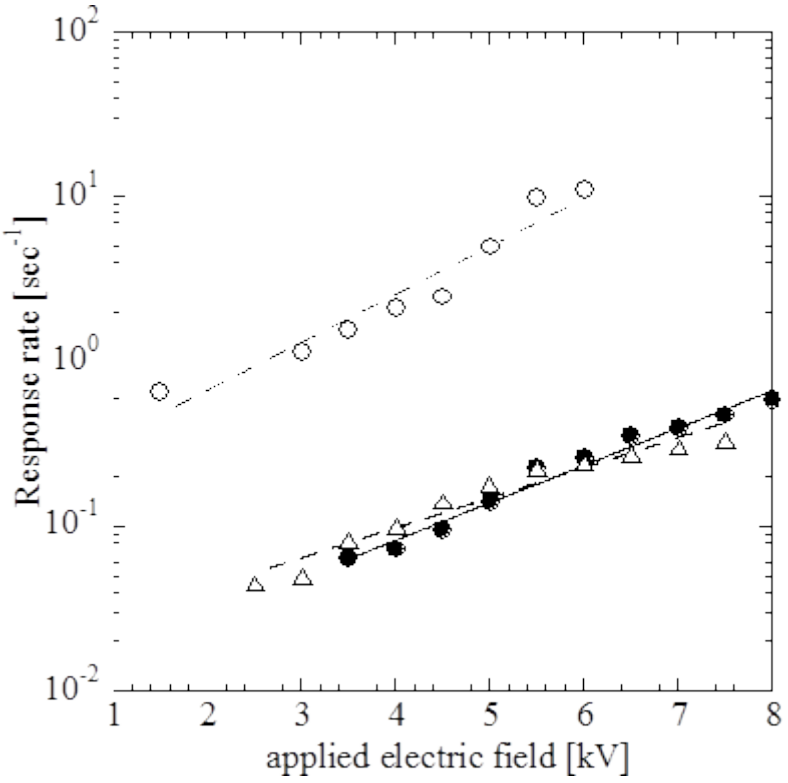

Fig. 5.7 Dependencies of applied electric field on response rate.
Filled and open circles represent response rates for devices based on P-TH-BisA / DEANST (70 / 30) and P-THEA /DEANST (70 / 30), respectively. Open triangle represents that of P-TH-BisA / DEANST (80 / 20).

5.3.5 Device Stability

In this study, we investigated PR properties for composites containing 30 wt% of EO chromophore, DEANST. For comparison, we fabricated the device based on conventional hole transporting poly(vinyl carbazole) (PVK) and DEANST with the same composition, and crystallization and phase separation of DEANST were observed in a week after the measurement. However, as reported in a previous paper for P-THEA based composite[4], P-TH-BisA composite also exhibited the superior temporal stability. Optical quality of devise based on P-TH-BisA/DEANST (70/30) maintained without crystallization and/or phase separation at room temperature 3 months after the measurement. Although the electron accepting nature of P-TH-BisA is weaker than that of P-THEA, the charge transfer interaction between electron accepting P-TH-BisA and electron donating DEANST still exist as mentioned above, and this interaction improved the temporal phase stability.

5.4. Conclusion

Poly(arylene ether) (P-TH-BisA) containing electron accepting thioxanthene unit was synthesized and characterized as a photorefractive host polymer. Compared with polyacrylate containing thioxanthene (P-THEA), lowered electron accepting nature afforded suppressed the absorption at 633 nm for the composite with electro donating DEANST, EO chromophore. Although the charge transfer interaction between P-TH-BisA and DEANST was weaker, it still worked as photocarrier generator and improved the temporal phase stability. Lower absorption afforded several advantages such as the larger net gain, and high external diffraction efficiency. Slower response was also attributed to the lower absorption resulting in poor photocarrier generation efficiency.

REFERENCES

1) J.-H. Sim, Y. Pei, K. Ogino, H. Sato, *J. Imaging Sci. Technol.*, **40**, 164 (1996)

2) H. Sato, Y. Sakaki, K. Ogino, Y. Ito, *Polym. Adv. Technol.*, **8**, 454 (1997)

3) H. Sato, H. Matsuda, K. Okamoto, K. Ogino, *Synth. Met*. **105**, 55 (1999)

4) K. Okamoto, T. Nomura, K. Ogino, H. Sato, *Chem. Mater.,* **11**, 3279 (1999)

5) R. Viswanathan, B. C. Johnson, J. E. McGrath, *Polymer*, **25**, 1827 (1984)

6) K. Ogino, H. Sato, K. Tsuchiya, H. Suzuki, S. Moriguchi, *J. Chromatogr. A*, **699**, 59 (1995)

7) Y. Zhang, Y. Cui, P. N. Prasad, *Phys. Rev. B*, **46**. 9900 (1992)

Chapter 6 General Conclusions

The author synthesized an electron-transporting polymer that is transparent in the visible region and has the requirements for electrophotography and photorefractive materials. It is found that high mobility depends on the uniformity of LUMO, which contributes to electron conduction, rather than on the magnitude of the reduction potential.

He also synthesized an amphoteric charge-transporting polymer using the Friedel–Crafts reaction. Synthesis of amphoteric charge-transporting and fluorescent multifunctional polymers using chemical oxidative coupling reactions, and application to organic electroluminescent devices. Thioxanthene unit is an aromatic system with electron withdrawing group (sulfoxy and carbonyl). It is found that dichloride monomer can be applied for a nucleophilic substitution polymerization. The resulting poly(arylene ether) can be utilized as a host polymer for photorefractive composites.

The author suggests that simple synthetic strategies (radical, condensation based on Friedel-Crafts reaction, and oxidative coupling) provide the high performance and multifunctional electron transporting polymer.

List of publications

1. Hisaya Sato, Hisaaki Matsuda, Kazuo Okamoto, Kenji Ogino, Yuanhu Pei, Synthesis and characterization of electron transporting polymers having thioxanthene derivatives, *Synthetic Metals*, **105**, 55-60 (1999) (Chapter 2)

2. Takeshi Washizu, Yuanfu Pei, Jaekook Ha, Martin Vacha, Kunio Tani, KenjiI Ogino, Hisaya Sato, Preparation of Polymers Having Hole and Electron Transport Units by Friedel–Crafts Reaction, *Journal of Polymer Science: Part A: Polymer Chemistry*, **45**, 3083–3089 (2007) (Chapter 3)

3. Pei Yuanfu, Masahisa Otake, Martin Vacha, Hisaya Sato, Synthesis and Characterization of a Novel Electroluminescent Polymer Based on Phenoxazine and Fluorene Derivatives, *Reactive & Functional Polymers*, **67**, 1211–1217 (2007) (Chapter 4)

4. Mototora Kai, Haruki Fukushima, Kazuo Okamoto, Kenji Ogino, Synthesis of Polymer having Thioxanthene Unit in Main Chain and Application to Photorefractive Composites, *Journal of Fiber Science and Technology,* accepted (Chapter 5)
(Yuanhu Pei; the name before naturalization)